A new approach for simulating the redistribution of soil particles by water erosion: A marker-in-cell model

James R. Cooper,[1] John Wainwright,[2] Anthony J. Parsons,[3] Yuichi Onda,[4] Tomomi Fukuwara,[4] Eiichiro Obana,[4] Ben Kitchener,[3] Edward J. Long,[5] and Graham H. Hargrave[5]

Received 24 May 2012; revised 19 September 2012; accepted 21 September 2012; published 6 December 2012.

[1] There are currently no process-based approaches that allow detailed spatial information on soil redistribution on hillslopes to be modeled at spatial scales that are appropriate for studying slope processes. In response, we developed a new type of soil-erosion model, a marker-in-cell model, which simulates the redistribution of soil during rainfall events. The model is a hybrid of cell- and particle-based techniques. A cell-based model is used to determine the hydrology and hydraulics occurring at the cellular scale on the hillslope. Markers, representing sediment, are then moved through the grid according to these properties. The spatial pattern of erosion is determined directly by the properties of the markers. The model allows two-dimensional spatial patterns of individual particle movement on a hillslope to be simulated within a computationally efficient framework. We have tested the model using data collected from a plot-scale, rainfall-simulation experiment. We measured the redistribution of ^{137}Cs-rich tracer soil to resolve the spatial patterns of erosion caused by a single, high-intensity, rainfall event. The model was able to recreate the key temporal and spatial aspects of the hydrology and hydraulics occurring on the plot, as well as the spatial redistribution of ^{137}Cs-rich tracer soil. The development of the model was used to probe our understanding of how to investigate soil-erosion processes. The lack of empirical underpinnings of the different model components highlighted the need to understand the spatiotemporal dynamics of soil erosion processes at the grain-scale so to provide a better process-based understanding of detachment and transport can be sought.

Citation: Cooper, J. R., J. Wainwright, A. J. Parsons, Y. Onda, T. Fukuwara, E. Obana, B. Kitchener, E. J. Long, and G. H. Hargrave (2012), A new approach for simulating the redistribution of soil particles by water erosion: A marker-in-cell model, *J. Geophys. Res.*, *117*, F04027, doi:10.1029/2012JF002499.

1. Introduction

[2] Predicting rates of soil erosion by water, and the consequent spatial distribution of erosion and deposition, is useful for determining the sustainability of agricultural practices, informing policy on erosion control, understanding river and reservoir sedimentation, estimating the runoff of contaminated soils and determining long-term hillslope – and consequently, landscape – evolution. A range of approaches has been taken to understand spatial patterns of soil erosion, from 1-D sediment-transport models [e.g., *Furbish and Haff*, 2010; *Heng et al.*, 2011] to simulating the movement of individual sediment particles [e.g., *Lisle et al.*, 1998; *Tucker and Bradley*, 2010]. As *Durrett and Levin* [1994, pp. 363–364] put it "one of the fundamental issues in the modeling of any system is the choice of the level of detail. The relevance goes far beyond mathematical convenience to the heart of understanding the mechanisms, specifically, which details at one level are important to the determination of phenomena at other levels and which can be ignored. In modeling the temporal evolution of a spatially distributed system…one can choose several levels of description involving different levels of spatial detail." This argument is particularly relevant to the modeling of hillslope processes because of the range of spatial and temporal scales over which they act. The processes of erosion, transport and deposition occur at the grain-scale but can produce landscape features at spatial and temporal scales several orders of magnitude larger. Computationally it is not possible currently both to model these

[1]Department of Geography and Planning, School of Environmental Sciences, University of Liverpool, Liverpool, UK.
[2]Department of Geography, Durham University, Durham, UK.
[3]Department of Geography, University of Sheffield, Sheffield, UK.
[4]Graduate School of Life and Environmental Sciences, University of Tsukuba, Tsukuba, Japan.
[5]Wolfson School of Mechanical and Manufacturing Engineering, Loughborough University, Loughborough, UK.

Corresponding author: J. R. Cooper, Department of Geography and Planning, School of Environmental Sciences, University of Liverpool, Liverpool L69 3GP, UK. (james.cooper@liverpool.ac.uk)

0148-0227/12/2012JF002499

grain-scale processes explicitly and to simulate a suitably large area to capture their large-scale behavior.

[3] A common approach in modeling soil erosion on hillslopes is to represent the continuum of spatial scales that are available to the modeler and subdivide the space into patches, creating a cell-based model [e.g., *Wright*, 1987; *Johnson et al.*, 2000; *Su et al.*, 2003; *Wainwright et al.*, 2008a]. These models have received particular attention because they reproduce plot-scale behavior from the simulation of sediment transfer between cells. Each grid cell is assumed to be homogenous and the small-scale processes occurring within each grid cell are not (usually) explicitly modeled and so are subject to some form of empirical parameterization. Sediment transport is dealt with using mathematical expressions that represent the average behavior of the particles contained within the cell, which are also parameterized by the grid-cell properties. Implicit is that the cellular (averaging) area is large enough that the difference in particle behavior within a cell is not significant but not so large that it smoothes out any emergent, larger scale dynamics, and is comparable to the concept of a representative elementary area/volume [e.g., *Wood et al.*, 1988; *Blöschl et al.*, 1995]. This discretization makes cell-based models computationally efficient, and a powerful method for simulating spatial patterns and furthermore it offers the potential to be a practical tool for landscape management.

[4] The discretization into grid cells has a number of limitations however. First, the resolved spatial scale of erosion is determined by the cell size rather than by the properties/behavior of the particles being modeled. Second, the resolved spatial scale of erosion does not relate to the "real" spatial scales of movement, therefore transport distance is not perfectly scaled. Measurements of travel distances of individual particles during run-off events show that these transport distances are small [*Parsons et al.*, 1993], inversely related to particle size [*Wainwright and Thornes*, 1991; *Parsons and Stromberg*, 1998] and have a negative exponential or gamma distribution [*Wainwright and Thornes*, 1991; *Parsons et al.*, 1993]. Thus, only the smallest eroded particles, or a fraction of larger ones, are likely to transported large distances, after even a very large run-off event. This evidence implies that the quantity of soil eroded from an area is not directly proportional to the size of the area [*Parsons et al.*, 2004]. Thus, the inherently (and implicitly) linear scaling of transport distance by most cell-based models means that soil erosion rates cannot be estimated accurately over a range of scales [*Wainwright et al.*, 2008a, 2008c]. Third, sediment-transport pathways do not necessarily follow the structure prescribed by the regular grid that is generally employed. The spatial patterns of erosion are dependent upon the cell size [*Wainwright et al.*, 2008c], cell shape and the geometrical arrangement of the cells. Fourthly, choosing the appropriate cellular frame is problematic. Very little is known about the cell size, cell shape and their geometrical arrangement for the variation in particle behavior within a cell to be considered "insignificant" and for spatial patterns of erosion to become independent of the cellular framework. Often the cell size is chosen based on some interpretation of the size of the representative elementary area for the system [*Wood et al.*, 1988]. However, given that a model will often be applied to a hillslope environment in which no data has been previously collected, it can be problematic to choose an appropriate cell size. Fifthly, cell-based models cannot represent fully the grain-scale processes of sediment transport. Particle movement on hillslopes is a stochastic process [e.g., *Wainwright and Thornes*, 1991; *Lisle et al.*, 1998; *Furbish et al.*, 2007]. Unless one can make a large-number approximation and ignore the spatial patterns of erosion, the assumption that all particles within a cell behave according to the mean is therefore not appropriate, particularly as one moves to smaller resolutions and bigger particles. This issue has long been recognized in the fluvial literature [e.g., *Einstein*, 1937], and the notion that sediment transport is a continuous process and can described by relationships between mean values has been discredited by many; a large number of stochastic modeling approaches have been used, dating back many years [e.g., *Einstein*, 1937; *Hubbell and Sayre*, 1964; *Paintal*, 1971; *Ancey*, 2010]. Within the hillslope literature, little effort has been made to describe runoff sediment dynamics in this way despite particle-based measurements of soil erosion that show that there is a continuum between slope and fluvial processes. For example, empirical observations suggest erosion in interrill flow is dominated by rolling and sliding along the surface, or in short steps akin to the movement of bed load [*Wainwright and Thornes*, 1991; *Parsons et al.*, 1993, 1998; *Rejman et al.*, 1999], and that in rills and gullies, bed load can make up a significant proportion of the sediment in transport [*Torri et al.*, 1990]. Finally, there is no spatial information contained within the cells on the location of particles. This lack of information means that all particles in a cell have an equal probability of being entrained irrespective of when they got there or where they have come from. This assumption does not accord with observation [e.g., *Wainwright and Thornes*, 1991; *Parsons et al.*, 1993], nor with the argument that the probability of detachment is dependent upon whether the particle resides in the deposited layer or in the unshielded, original soil layer [*Hairsine and Rose*, 1992a, 1992b].

[5] A particle-based understanding of soil erosion is of particular importance for understanding the movement of contaminated sediment and the sources of sediment to rivers and reservoirs. In previous cell-based and one-dimensional approaches, the movement of individual particles has not been tracked so the sources and sinks of soil particles are not known. Thus if a greater understanding is to be gained of the processes of soil erosion, a different approach is required to modeling the redistribution of soil. More generally, given the attention paid to spatial testing of hillslope soil erosion models, and the recognition that simply evaluating against the slope hydrograph (or sedigraph) provides an insufficient test of adequate representation of behavior within the plot [*Parsons et al.*, 1997; *Beven*, 2001], alternative strategies are required for model evaluation. One approach is to use particle-tracking measurement techniques, but in the case where no information is available in the model on particle location, these promising new techniques [e.g., *Furbish et al.*, 2007; E. J. Long et al., New insights into the mechanisms of splash erosion using highspeed, three dimensional, particle tracking velocimetry, manuscript in preparation, 2012] cannot be used.

[6] An alternative to the cell-based approach is going to the opposite side of the scale spectrum and use particle-based models to simulate the movement of individual grains. One type of model that is starting to receive a good deal of attention within geomorphology is the Discrete Element Model [e.g.,

McEwan and Heald, 2001; *Calantoni et al.*, 2004; *Kang*, 2012], which involves creating a 'numerical' deposit of sediment grains with a given size and density. The forces acting on each of these grains are calculated, including the gravity force, contact forces between the grains, and the fluid force acting on their surface. The resultant force is used to determine if the grain is entrained. Once entrained, the velocity of the grain is modified by a fluid model and the collisions it makes with other mobile and static grains. If enough of these particles are simulated, the assumption is that their aggregated behavior will facilitate understanding of larger-scale behavior. The approach allows the processes of sediment transport to be modeled explicitly, as well as allowing the movement and subsequent redistribution of individual sediment particles to be tracked.

[7] However, such models are computationally demanding and are restricted to small-scale and short-duration applications. The position, velocity and direction of each particle must be tracked, the particle pair that creates the next collision must be detected, and the collisional behavior needs to be resolved. This myriad information limits the slope area, run duration and sediment grain-size distribution of the model because there is a geometric increase in computational requirement. In 2-D simulations, as the linear scale increases, the number of particles that need to be simulated, N_p, increases as the square of the distance, and in fully 3D simulations N_p increases as the cube. The problem can be defined by $\sim N_p^{FL}$, in which F is the number of resolved forces (and particle interactions) and L is the dimensionality of the simulation (two or three). An increase in N_p means that the time step must reduce to ensure that single collisions occur within a time step and hence the computing time increases significantly. This increase is a particular problem at higher transport rates because more grains are in motion, hence there are more inter-grain collisions, so the time step has to be shortened and the computational time lengthened. Furthermore, an increase in the range of particle sizes also increases the run time because there will be more contacts between particles. Consequently, Discrete Element Models are not currently suitable to examine large-scale patterns of soil redistribution and landscape evolution on hillslopes.

[8] A far simpler technique is to ignore the effects of inter-particle interaction and model grain motion statistically. *Lisle et al.* [1998] and *Tucker and Bradley* [2010] viewed sediment motion as an alternating process of rest and motion (hops), each with associated probability-density functions. This work drew upon a well-established stochastic approach in the fluvial literature [e.g., *Einstein*, 1937; *Hubbell and Sayre*, 1964; *Paintal*, 1971]. The authors demonstrated the approach was a highly efficient method (computationally more efficient than 1D linear or nonlinear diffusion equations) and able to capture local and non-local sediment dynamics and the larger-scale patterns of landform evolution. However, these models were untested, only able to simulate transport occurring in the downslope direction – providing limited information on the spatial distribution of erosion and deposition – and did not account for the full range of sediment detachment and transport processes.

[9] In summary, there are currently no process-based approaches that allow detailed spatial information on soil redistribution to be modeled at spatial scales that are appropriate for studying slope processes. Thus, in response to these shortcomings, we propose a hybrid of the approaches discussed above; a marker-in-cell (MiC) model of soil erosion. We evaluate this model and illustrate its capabilities by comparing its performance against data obtained from a large, rainfall-simulation experiment for which the redistribution of soil has been mapped. In so doing, we use the model to highlight current limitations in our understanding of soil-erosion processes.

[10] The MiC model combines a cell-based approach with a particle-based approach to simulate the movement of individual sediment particles within a computationally efficient framework. Markers (representing sediment particles), containing sediment-property information, are initially distributed on a cellular grid. A cell-based model is used to set up the boundary conditions and determine the hydrology and hydraulics occurring at the cellular scale on the hillslope. The markers are then moved, independent of one another, through the grid according to these properties. Figure 1 provides an overview of the approach. The model simulates all the processes of detachment and transport and allows erosion to be treated in a fully stochastic, but simple, manner. The spatial pattern of erosion is determined directly by the properties of the markers rather than by the properties of the cellular framework.

[11] The approach combines the advantages of Eulerian and Lagrangian methods while avoiding the shortcomings of each (computational efficiency versus accuracy). In so doing, it allows large numbers of markers to be accommodated and for particle behavior to be resolved over scales that are useful for understanding landscape evolution and the redistribution of soil in the context of river and reservoir sedimentation.

[12] The MiC model is inspired by the particle-in-cell (PiC) approach developed by *Harlow* [1957] for modeling fluid flow, and used since to investigate flows like plasma flow [e.g., *Butler et al.*, 1969], supersonic flows [e.g., *Brackbill and Ruppel*, 1986], and atmospheric [e.g., *Lange*, 1978] and oceanic flows [e.g., *Pavia and Cushman-Roisin*, 1988]. The two approaches are similar because both use a Lagrangian coordinate system superimposed upon an Eulerian one, and a cellular grid to resolve the flow field to move the particles/markers. They are different, however, in the way in which the Lagrangian and Eulerian components of the model interact. In PiC, the space occupied by the fluid is represented by a network of cells. For each time step, fluid momentum equations are solved at the grid scale to resolve the fluid velocity in each of the cells. The fluid within these cells is represented by particles, each of which carries a fixed mass of fluid. The velocities of the particles are resolved by interpolation of the velocity field from the cellular grid to the particles, and the particles are then moved through the grid. The particle positions are used to interpolate the fluid mass of the particles onto the cellular grid, resulting in the routing of fluid mass through the cellular grid. Thus, in PiC there is transfer of information back and forth between the particles and the grid at every time step, whereas in MiC there is no two-way interaction – the conditions within the cellular grid drive the movement of the markers. We are not aware of the MiC approach being used to model sediment transport within the field of soil erosion.

2. Model Structure

[13] The cellular component of the model utilizes an existing cell-based model – MAHLERAN (Model for Assessing

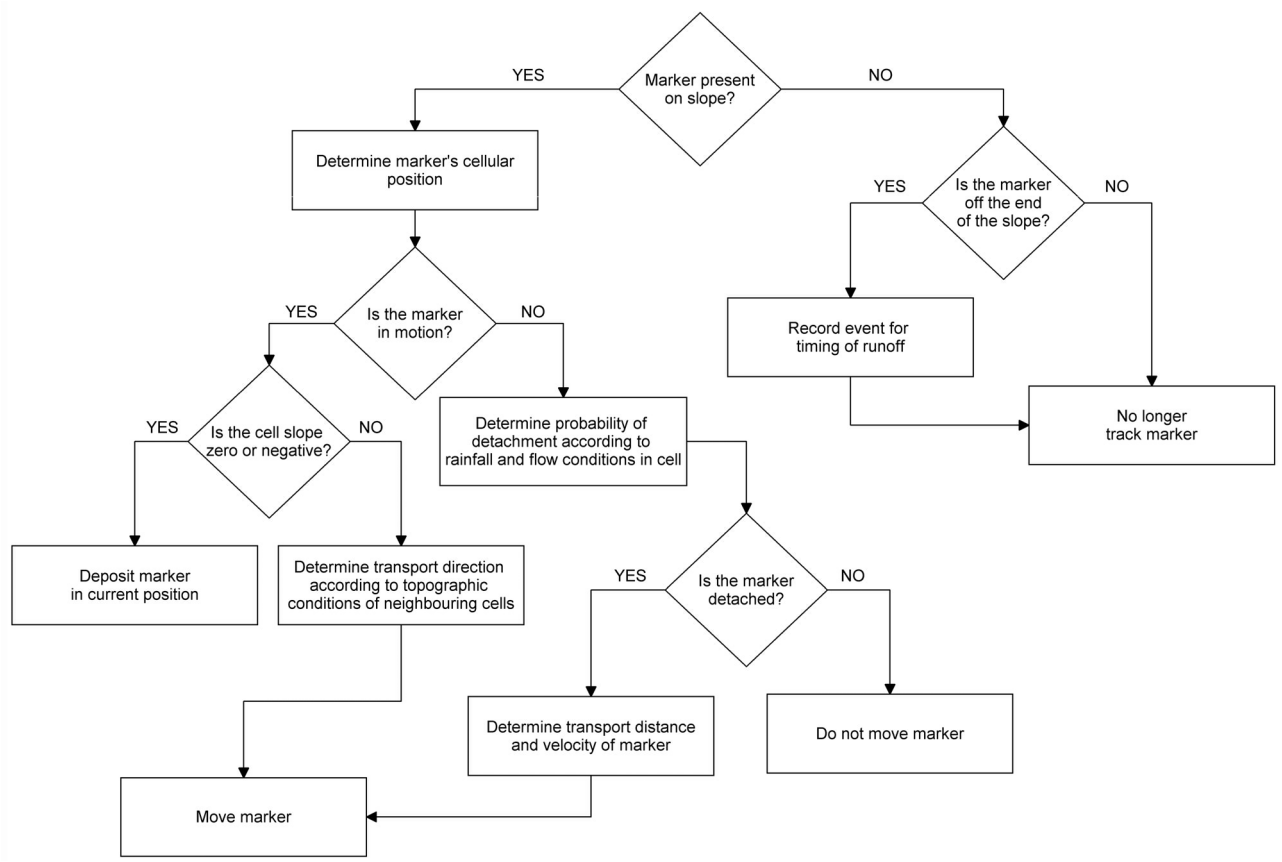

Figure 1. An outline of the marker component of the MiC model, also illustrating how the markers interact with the cellular component of the model.

Hillslope to Landscape Erosion, Runoff And Nutrients) – detailed information about which can be found in *Wainwright and Parsons* [2002], *Wainwright et al.* [2008a, 2008b], *Müller et al.* [2007] and *Turnbull et al.* [2010]. The model is based on a two dimensional finite difference grid and is coupled with a simple infiltration model to generate infiltration- and saturation-excess runoff. Infiltration-excess runoff is generated by determining the difference between the rainfall rate and the infiltration rate. The infiltration rate is simulated using the Smith-Parlange approach [*Smith and Parlange*, 1978]. Overland flow is routed over the hillslope by means of a kinematic wave approximation of the St. Venant equations, with flow routing in the direction of steepest descent from cell to cell (in cardinal directions). The flow is routed over the grid using a finite difference solution (Euler backward difference form [*Scoging*, 1992]). In *Tatard et al.* [2008] we compared our kinematic wave approximation against full shallow-wave solutions and found it to be a reasonable approximation, especially when the computational overheads involved are considered. Flow velocity is determined dynamically using the Darcy-Weisbach flow equation. The flow sub-model has been intensively tested in a range of conditions by *Scoging et al.* [1992], *Parsons et al.* [1997], *Müller et al.* [2007], *Tatard et al.* [2008] and *Turnbull et al.* [2010], enabling our confidence in its broad applicability.

[14] The sediment-detachment, transport and deposition components of the existing version of MAHLERAN are not used but are replaced with explicit particle-based methods. The MAHLERAN-MiC version works by initially distributing a given number of markers within a set of chosen cells. The markers are assigned a location, size and density, and when moved, an initial velocity. At each time step the rainfall, hydrology and hydraulics are solved for each cell and the cellular position of each marker is determined. The markers are entrained or transported according to these conditions, and, if transported a sufficient distance, by the topographic properties of the neighboring cells. The movement of each marker is tracked through each time step. The virtual velocity (distance moved per time step) of the marker is related to the time step of the cell-based model.

[15] The mode of detachment and transport of a marker is governed by the rainfall and hydraulic conditions. Each process is modeled separately since the relative balance of the different processes is the most critical control on the resulting pattern of erosion [*Wainwright et al.*, 2008b]. A marker can be detached by raindrop impact, unconcentrated flow or concentrated flow (as bed load or into suspension) and transported via rain splash, interrill flow and concentrated flow (bed load and suspended transport). Figure 2 outlines the definitions of these processes and how they combine in different rainfall and overland flow conditions. Our aim, where possible, is to parameterize the processes based on data sources that cover a wide range of soil, slope and rainfall conditions so that the model can be utilized in a wide range of conditions in

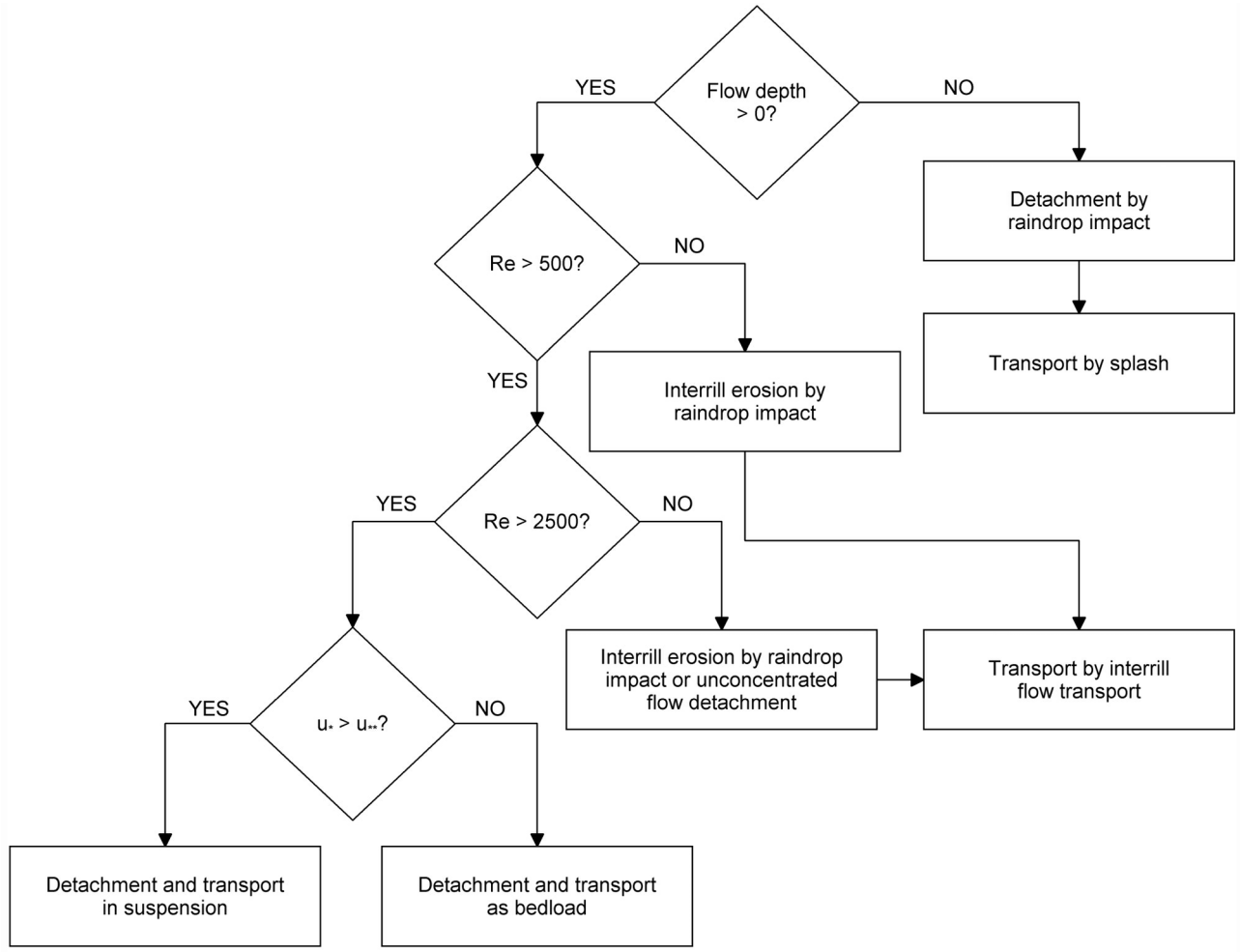

Figure 2. Definition of detachment and transport processes.

uncalibrated form. The next section of the paper will describe, in detail, the manner in which each of these processes is simulated.

3. Model Components

3.1. Raindrop Detachment

[16] At times or in locations where no flow is present, the markers are detached by raindrop impact. We are not aware of any study that has produced a particle-based, probability-distribution function of detachment. Thus, we use the cell-based, stochastic model of raindrop detachment developed by *Wright* [1987] to estimate the probability of detachment for individual markers. For a given cell, *Wright* [1987] estimated the probability of an individual particle being detached based on the bulk sediment and transport properties of all the particles residing in the cell, and as such his model is not a true MiC model. To explain our approach, consider a marker belonging to a size class φ and occupying a particular cell. The probability of a marker of this size class being detached ($P_{r,\varphi}$) due to a raindrop falling at its location is equal to the ratio of the mass of particles splashed ($M_{r,\varphi}$) within the entire cell to the mass of particles available for splashing:

$$P_{r,\varphi} = \frac{M_{r,\varphi}}{\rho_s l_x^2 h_s} \cdot \frac{n_\varphi}{N_\varphi} \tag{1}$$

where ρ_s is the sediment density [kg m^{-3}], l_x is the length of the side of a single cell [m], h_s is the available depth of soil for detachment [m], n_φ is the proportion by mass of splashed soil particles [−] and N_φ is the proportion by mass of soil particles [−] in the size class φ present on the hillslope. The detached mass is parameterized using the results of *Quansah* [1981], whose approach is the only approach to our knowledge that allows different rates of detachment to be calculated as a function of particle size, rainfall kinetic energy and surface slope [see *Wainwright et al.*, 1995]:

$$\varepsilon_{r,\varphi} = a_\varphi \mathrm{KE}^{b_\varphi}, \quad S = 0 \tag{2a}$$

$$\varepsilon_{r,\varphi} = a_\varphi \mathrm{KE}^{b_\varphi} S^{c_\varphi}, \quad S > 0 \tag{2b}$$

where $\varepsilon_{r,\varphi}$ is raindrop detachment for particle size class φ [kg m^{-2}], KE is rainfall kinetic energy per unit area per unit precipitation [J m^{-2} mm^{-1}], S is surface slope [m m^{-1}], and a_φ, b_φ, c_φ are empirical parameters that are functions of particle size and density. Since the experimental procedure used by *Quansah* [1981] involved collecting splashed sediment in only the upslope and downslope directions (assuming an infinitely wide source [cf. *Savat and Poesen*, 1981]), $\varepsilon_{r,\varphi}$ is doubled to give the total, two-dimensional detachment rate. It is likely that parameters a_φ, b_φ, c_φ will vary dynamically according to changes in soil cohesion [*Kinnell*, 1974; *Al-Durrah and Bradford*, 1982; *Nearing and Bradford*, 1985; *Bradford et al.*, 1987b], surface sealing [*Bradford et al.*, 1986, 1987a], aggregate stability [*Farres*, 1987], organic matter content [*Tisdall and Oades*, 1982], soil compaction [*Drewry et al.*, 2004] and particle arrangement [*Torri*, 1987], but at present there are insufficient empirical data for the parameterization of these dynamics, so they are not included in the current model (see further discussion by *Wainwright et al.* [2008c]). Where vegetation is present, the kinetic energy is scaled to account for changes in energy relating to interception losses, throughfall and leaf drip using a simplified derivation of the measurements made by *Wainwright et al.* [1999].

3.2. Rain Splash Transport

[17] If a marker is entrained via raindrop impact and no flow is present the marker is transported via rain splash transport following the theoretical approach of *Furbish et al.* [2007]. *Furbish et al.* [2007] used high-speed photography and plan view photographs to measure the transport of individual grains under dry soil conditions (grain diameter = 0.18 mm, 0.35 mm, 0.84 mm). Their data showed that the radial travel distance approximated an exponential distribution, confirming previous empirical observations [*Mosley*, 1973; *Savat and Poesen*, 1981; *Riezebos and Epema*, 1985; *Torri et al.*, 1987], and radial plots of final ejected grain positions displayed an increasing slope-dependent asymmetry with increasing slope. Using these data, and a theoretical argument that the radial angle of transport is related to the spatial redistribution of momentum of the deforming raindrop on impact, *Furbish et al.* [2007] developed a model for the probability of a splashed particle's being deposited in a given location. We use this model to estimate the joint probability density of radial splash distance $L_{s,\varphi}$ [m] and radial angle θ [radians]:

$$f\left(L_{s,\varphi},\theta\right) = \frac{f(\theta)}{\langle L_{s,\varphi}\rangle(\theta)} \exp\left(\frac{-L_{s,\varphi}}{\langle L_{s,\varphi}\rangle(\theta)}\right), \quad -\pi \le \theta \le \pi \tag{3}$$

in which $\theta = 0$ is the downslope direction. We estimate the mean distance $\langle L_{s,\varphi}\rangle$ by $1/\alpha_\varphi$, in which α_φ [m] is an empirical constant taken from *Savat and Poesen* [1981]. In equation (3) the probability-density function for radial angle is given by [*Furbish et al.*, 2007]:

$$f(\theta) = \frac{\Gamma^2}{2\pi}\left(\cos^2\theta - \sin^2\theta\right) + \frac{\Gamma}{\pi}\cos\theta\sqrt{1-\Gamma^2\sin^2\theta} + \frac{1}{2\pi}, \quad -\pi \le \theta \le \pi \tag{4}$$

where $\Gamma = |u_s|/|u_n| \sim \tan\beta$, in which β is the surface slope angle, u_s is the downslope component of the surface-parallel velocity of the impacting raindrop and u_n is the slope-normal component. The parameter Γ accounts for the effect of slope on the radial angle by reflecting the change in the radial redistribution of momentum of the deforming raindrop with slope. With increasing values of Γ the radial redistribution of momentum (splashed particles) becomes increasingly asymmetrical in the downslope direction. In our model, transport is assumed to occur within one time step since we are not aware of any study that has measured splashed particle velocities (although this is the focus of a paper by the authors E. J. Long et al. (manuscript in preparation, 2012)). The assumption is reasonable for time steps that are greater than the duration of a single splash event (~0.1 to 0.2 s) (E. J. Long et al., manuscript in preparation, 2012), and so applicable to the timescales needed to simulate landscape change.

3.3. Interrill Erosion by Raindrop Impact

[18] In locations or at times in which there is overland flow present but not at a sufficiently high shear stress to entrain the sediment, detachment occurs via raindrop impact [*Kinnell*, 1990, 1993]. Raindrop detachment is estimated using the method described in section 3.1, modified to account for the protective effects of the surface water layer. The exponential model of *Torri et al.* [1987] provides this modification, but accounting for the parameterization issue noted by *Parsons et al.* [2004]:

$$\varepsilon_{i,\varphi} = \varepsilon_{r,\varphi} e^{-\beta_\varphi h_w} \tag{5}$$

where $\varepsilon_{i,\varphi}$ is interrill raindrop detachment rate [m s^{-1}] for a flow depth h_w [m], and β_φ is an empirical parameter reflecting the changing energy arriving at the surface with increasing flow depth (relative to the diameter of a particle of size class φ).

3.4. Interrill Erosion by Raindrop Impact or Unconcentrated Flow Detachment

[19] These conditions are taken to occur when the flow Reynolds number falls in the range $500 \le \mathrm{Re} < 2500$, corresponding to partial turbulence in the transitional flow régime. This situation is likely to reflect conditions where ponding has occurred but flow connectivity is not fully developed and/or the surface slope is low. Detachment can occur either by raindrop impact, as described above, or through detachment by unconcentrated flow, with the latter occurring when the flow depth becomes too large for a raindrop to have sufficient kinetic energy to entrain a grain on the sediment surface. Raindrop detachment is estimated using the approach outlined above for interrill erosion and the erosion by unconcentrated flow is estimated using the probabilistic approach of *Einstein* [1942], which has been subsequently modified by *Wu and Lin* [2002]. The probability that a marker is detached via flow in these conditions ($P_{f,\varphi}$ [−]) is given by:

$$P_{f,\varphi} = 0.5 - 0.5\frac{\ln\left(0.049/0.25U_{*,\varphi}\right)}{\left|\ln\left(0.049/0.25U_{*,\varphi}\right)\right|} \cdot \sqrt{1 - \exp\left(-\frac{2}{\pi}\left[\frac{\ln\left(0.049/0.25U_{*,\varphi}\right)}{0.702}\right]^2\right)} \tag{6}$$

where $U_{*,\phi}$ is the dimensionless flow shear velocity [−], defined by $U_{*,\varphi} = u_*^2/(\sigma d D_\varphi)$, u_* is the flow shear velocity [m s^{-1}] calculated by $u_* = \sqrt{g h_w S}$, σ is the specific sediment density [−] calculated as $\sigma = (\rho_s - \rho)/\rho$, D_φ is the marker diameter [m] and ρ is water density [kg m^{-3}].

3.5. Interrill Flow Transport

[20] In interrill flow conditions, once a marker is entrained due to either raindrop impact or unconcentrated flow detachment, the marker is transported by unconcentrated flow [*Kinnell*, 2001]. The marker's travel distance is simulated using an exponential distribution parameterized by the mean travel distance $\langle L_{u,\varphi} \rangle$ [m] calculated as:

$$\langle L_{u,\varphi} \rangle = 0.05 K E^{1.85} \omega^{0.481} M_{p,\varphi}^{-0.425} \tag{7}$$

where $M_{p,\varphi}$ is particle mass [g], ω is overland flow energy or stream power [J m^{-2} s^{-1}], calculated as $\omega = g h_w u S$, in which g is acceleration due to gravity [m s^{-2}] and u is flow velocity [m s^{-1}]. Equation (7) is derived from a reanalysis of data presented by *Parsons et al.* [1998], in which the travel distances of particles in low Reynolds number, rain-impacted flows were measured. They also found that the particle velocity followed an exponential distribution and that it can be parameterized by the median velocity $u_{p,\varphi}$ [cm s^{-1}]:

$$u_{p,\varphi} = \frac{8.75 \times 10^{-5} K E^{2.35} \omega^{0.981}}{M_{p,\varphi}}. \tag{8}$$

The marker's travel velocity is estimated from this exponential distribution. Unlike the rain splash model, in which the duration of transport is very small, interrill flow transport is not assumed to occur instantaneously – the duration of motion is obtained according to estimates from the exponential distribution functions of travel distance and travel velocity.

3.6. Bed Load Detachment and Transport

[21] In concentrated flow where Re ≥ 2500 the detachment and transport processes can occur as either bed load or suspended load. The former is often neglected in soil-erosion models [see *Wainwright et al.*, 2008a]. On most hillslopes, transport in suspension rarely occurs for all but the finest particles, although these particles generally form aggregates that will exceed the threshold for motion unless these aggregates breakdown. Particles in interrill flow roll, slide or saltate [*Wainwright and Thornes*, 1991; *Parsons et al.*, 1993, 1998; *Rejman et al.*, 1999; *Kinnell*, 2012], and in rills, gullies and channels bed load can make up a significant proportion of the sediment in transport [*Guy et al.*, 1966; *Dietrich and Whiting*, 1989; *Torri et al.*, 1990; *Parker*, 2007]. We choose to use different detachment processes in these conditions because the movement of bed load and suspended load occur at different levels of shear stress.

[22] The *van Rijn* [1984] suspension criterion is used to determine whether the marker moves as bed load or in suspension. Suspension is deemed to occur if the flow shear velocity is greater than a critical value, defined as

$$u_{**,\varphi} = \frac{4 u_{s,\varphi}}{D_{*,\varphi}}, \quad 1 < D_{*,\varphi} \le 10 \tag{9a}$$

$$u_{**,\varphi} = 0.4 u_{s,\varphi}, \quad D_{*,\varphi} \le 10 \tag{9b}$$

where $u_{**,\varphi}$ is the critical shear velocity for suspension [m s^{-1}], $u_{s,\varphi}$ is the settling velocity of the marker [m s^{-1}], and $D_{*,\varphi}$ is the dimensionless particle size [−], defined as

$$D_{*,\varphi} = D_\varphi \left(\frac{(\sigma - 1) g}{\nu^2} \right)^{1/3} \tag{10}$$

where ν is the kinematic viscosity of water [m^2 s^{-1}].

[23] Bed load entrainment and transport is simulated using a random walk model. The markers are modeled as undergoing alternating states of rest and motion, as confirmed by observation [e.g., *Grass*, 1970; *Drake et al.*, 1988; *Wainwright and Thornes*, 1991; *Parsons et al.*, 1998; *Lajeunesse et al.*, 2010]. The random walk model is a development of the two-state continuous-time Markov chain models that have been widely used within the fluvial literature [e.g., *Papanicolaou et al.*, 2002; *Ancey et al.*, 2006], and used by *Lisle et al.* [1998] for soil erosion. As a first approximation we assume that the markers have no "memory"; marker motion is influenced only by its present state (rest or motion). Experimental observations by *Ancey et al.* [2006], revealed the time lags between motion and resting (entrainment), and between resting and motion (deposition) were virtually the same and shows that this assumption is reasonable for single flow events.

[24] Our model differs in two ways from previous approaches. First, rather than using a two-state continuous-time Markov chain model in which (necessarily) times in the resting and moving states are exponentially distributed, we treat the change in state as an alternating renewal process [*Cox*, 1962]. Thus the distributions for motion and rest duration are arbitrary and informed by observation rather than assumed to be exponential [*Cox*, 1962], which assumption, as we show below, only partially holds. Second, motion is not assumed to occur instantaneously, since motion time for particles in flow is much longer than when splashed. Markers are assigned a particle velocity according to estimates from the probability-density functions of travel distance and motion duration.

[25] Tagged particles have been used to examine the travel distance and virtual velocities of particles on hillslopes [*Poesen*, 1987; *Torri and Poesen*, 1988; *Wainwright and Thornes*, 1991; *Parsons et al.*, 1998], although these studies have generally used large particles. Likewise, there is a wealth of information in the fluvial literature on the travel distances and virtual velocities of tagged particles undergoing bed load transport [e.g., *Hassan et al.*, 1992; *Ferguson et al.*, 2002]. However, the data presented in these fluvial and hillslope studies often relate to movement over long temporal and large spatial scales when movement was sampled infrequently (e.g., before and after a flood or a rainfall event). It is not possible to determine whether the measured movement is due to single or multiple transport events, and therefore they do

not provide any information on the rest and motion durations and travel distance during a single entrainment event. We know of only one study [*Lajeunesse et al.*, 2010] that has parameterized how motion duration and travel distance changes with particle size and flow conditions at the time scales of motion. These authors observed the movement of gravels ranging in size from 1.15 mm to 5.5 mm within a laboratory flume under steady and uniform flow conditions. They found the "most probable" (undefined in the paper) motion duration to be well approximated by:

$$\langle t_{\mathrm{m},\varphi} \rangle = (10.6 \pm 0.7)\sqrt{\frac{D_\varphi}{\sigma g}} \tag{11}$$

where $\langle t_{\mathrm{m},\varphi} \rangle$ is the most probable motion duration [s], which we have taken to be the modal duration. The dimensionless motion duration had no clear variation with either $(u_* - u_{*,\mathrm{c}})/u_{\mathrm{s},\varphi}$ or $\mathrm{Re_s}$, where $u_{*,\mathrm{c}}$ is the critical shear velocity for bed load [m s^{-1}], $u_{\mathrm{s},\varphi}$ is the particle settling velocity [m s^{-1}] and $\mathrm{Re_s}$ is the settling Reynolds number [−]. An analysis of their data revealed that motion duration was well approximated by a lognormal probability distribution. Equation (11) is used to parameterize a lognormal distribution for motion duration.

[26] A similar approach is taken for modeling the distance traveled. A lognormal distribution also provided a good fit to the data of *Lajeunesse et al.* [2010]. They found that the most probable dimensionless travel distance increased linearly with excess shear velocity and could be estimated by:

$$\langle L_{\mathrm{m},\varphi} \rangle = (70 \pm 2)\frac{D_\varphi (u_* - u_{*,\mathrm{c}})}{u_{\mathrm{s},\varphi}} \tag{12}$$

where $\langle L_{\mathrm{m},\varphi} \rangle$ is the most probable travel distance [m].

[27] The estimation of rest duration is not so well constrained. *Papanicolaou et al.* [2002] recorded mean rest durations ranging from 0.38 to 0.75 s for the transport of single-sized spheres within a hydraulic flume. In a similar set-up, *Ancey et al.* [2006] measured shorter durations of 0.02 to 0.1 s. The short durations measured by these two studies imply much higher transport rates than are likely to occur on a hillslope. For example, in *Ancey et al.* [2006] these durations equate to transport rates of 23–90 kg m^{-1} s^{-1} that are orders of magnitude larger than observed transport rates in rills and gullies [e.g., *Zhang et al.*, 2008; *Wells et al.*, 2009]. Rather than using the rest durations in *Papanicolaou et al.* [2002] and *Ancey et al.* [2006] the rest duration is modeled based on the results of *Heays et al.* [2010] for two reasons. First, a wide range of sediment sizes was examined in a well-graded mixture (0.3 mm to 25 mm). Second, measurements were performed over a period of 6 h, in which the mixture was armoured under conditions of no upstream sediment input. Entrainment thresholds increased with time, so a range of levels of excess shear stress (and transport rate) was examined. *Heays et al.* [2010] found that the rest duration followed an exponential distribution and had a mean period of 14 s. We assume this distribution holds for all marker sizes and excess shear stress levels. We are not aware of any study that has examined how the shape and mean of the distribution changes with these two parameters, but it is likely that the mean will increase for larger particles and decrease with higher transport rates. The data of *Heays et al.* [2010] provide an aggregated result since they relate to the movement of a well-graded mixture over a range of levels of excess shear stress.

3.7. Suspended Detachment and Transport

[28] We are not aware of any studies that have measured the transport distance and velocity of particles in suspension in either the hillslope or fluvial literature. However, theoretical studies exist of suspension trajectories in aeolian transport that are physically based. A first approximation can be made by using such models and altering the physical parameters to account for the differences in the transporting media.

[29] *Anderson* [1987] produced an aeolian model which simulated the effects of turbulent fluctuations in vertical flow velocity on particles of varying size in suspension. We modify this model by introducing a new flow model which contains both a time-averaged and turbulence component, and modify the ejection conditions so that the model is fully stochastic in both detachment and transport.

[30] First, the vertical distribution of the time-averaged horizontal velocity $\bar{u}$ [m s^{-1}] is estimated using the log-law (equation (13a)) and log-wake law (equation (13b)) [*Nezu and Nakagawa*, 1993]:

$$u^+ = \frac{1}{\kappa}\ln y^+ + B - \Delta U^+, \quad y/h_{\mathrm{w}} \le 0.2 \tag{13a}$$

$$u^+ = \frac{1}{\kappa}\ln y^+ + B - \Delta U^+ + \frac{\Pi}{\kappa}2\sin^2\left(\frac{\pi y}{2h_{\mathrm{w}}}\right), \quad y/h_{\mathrm{w}} > 0.2 \tag{13b}$$

where u^+ is the dimensionless horizontal flow velocity [−], defined by $\bar{u}/u_*$, $\kappa = 0.41$ is the von Kármán constant [−], y^+ is the dimensionless height above the bed [−], defined by yu_*/ν, in which y is the height above the bed [m], $B = 4.9$ is the intercept for a smooth wall [−], ΔU^+ is the roughness function [−], Π is the Coles wake parameter [−] and h_{w} is the height of the water surface above the bed [m]. The roughness function represents the shift in the log-law due to bed roughness (relative to a smooth wall flow) and depends on the roughness Reynolds number k_{s}^+ [−], in which $k_{\mathrm{s}}^+ = k_s u_*/\nu$ and k_{s} is the bed roughness height [m], defined as $2D_{50}$, and D_{50} is the median particle diameter on the bed surface. Equations (13a) and (13b) hold for flows over a range of different roughness types [e.g., *Tachie et al.*, 2000; *Antonia and Krogstad*, 2001; *Bergstrom et al.*, 2001; *Balachandar and Patel*, 2002; *Schultz and Flack*, 2003; *Bigillon et al.*, 2006].

[31] Overland flows over fine sediments (up to fine gravels), and in conditions in which suspension occurs, most commonly fall within the transitionally rough regime where $5 < k_{\mathrm{s}}^+ < 70$. In this regime $2\Pi/\kappa = 0.5$ [*Bigillon et al.*, 2006] and the roughness function is given by:

$$\Delta U^+ = \frac{1}{\kappa}\ln k_{\mathrm{s}}^+ + 5.75 - 8.5 \tag{14}$$

This relationship has been shown to hold by many previous studies of open channel flows [e.g., *Schlichting*, 1979;

Bergstrom et al., 2001; *Schultz and Flack*, 2003; *Bigillon et al.*, 2006].

[32] Second, a temporal fluctuation in horizontal flow velocity, dependent on the height of the marker above the bed, is simulated using the semi-theoretical curve of *Nezu* [1977]:

$$u^+_{\mathrm{rms}} = \left(a \exp\left(-\frac{y^+}{\mathrm{Re}_*}\right)[1 - \exp(-y^+/b)] + cy^+ \exp(-y^+/b)\right) \quad (15)$$

where u^+_{rms} is the dimensionless turbulence intensity in the horizontal direction [−], defined by u_{rms}/u_*, in which u_{rms} is the standard deviation in horizontal flow velocity [m s^{-1}], Re_* is the flow Reynolds number [−], defined as $u_* h_{\mathrm{w}}/\nu$, and a, b and c [−] are empirical coefficients which change according to bed roughness (e.g., $a = 2$, $b = 8$ and $c = 0.34$ for sand beds) [*Bigillon et al.*, 2006]. Based on *Wu and Lin* [2002] and *Bigillon et al.* [2006] the temporal fluctuations in horizontal velocity are simulated to follow a lognormal distribution. The distributions are parameterized by $\bar{u}$ and u_{rms}.

[33] Third, the fluctuation in vertical flow velocity is adjusted according to height by the following relationship:

$$w^+_{\mathrm{rms}} = 1.14 \exp\left(-0.76 \frac{y}{h_{\mathrm{w}}}\right) \quad (16)$$

where w^+_{rms} is the dimensionless turbulence intensity in the vertical direction [-], defined by w_{rms}/u_*, in which w_{rms} is the standard deviation in vertical flow velocity [m s^{-1}]. Equation (16) holds for surfaces with a range of different grain-size compositions [e.g., *Kironoto and Graf*, 1994; *Song et al.*, 1994; *Bigillon et al.*, 2006].

[34] Fourthly, a distribution of possible ejection angles is used based on observations of aeolian transport. *Kang et al.* [2008] found the angle to follow an exponential distribution. Our analysis of the presented mean values revealed that they had little correlation with free-stream horizontal flow velocity and grain size. Accordingly we parameterize the exponential distribution by the mean of all the ejection angles (38.8°) measured by *Kang et al.* [2008].

[35] Finally, we model the ejection velocities (horizontal and vertical) using a normal distribution, based on the results of *Kang et al.* [2008]. This distribution is parameterized by the mean and standard deviation of all of their measured ejection velocities. A single trajectory is simulated for each marker and used to derive the motion duration and travel distance for a marker.

3.8. Marker Routing via Flow Transport

[36] Unlike a cell-based model, transport distances are perfectly represented. Markers can be transported within a cell, as well as outwith. The transport distance is not influenced by the cellular framework, only by the conditions at detachment. In each form of flow transport, if the transport distance is sufficient for the marker to leave its cell, the marker is routed to the adjacent cell with the steepest downslope gradient, its direction modified by the topographic properties of each successive cell it passes through as it is routed. The marker is deposited when either a cell with zero or positive bed slope is encountered or the duration of motion ends. Once in transport the mode of transport does not change, irrespective of the rainfall and flow conditions the marker encounters as it passes through the cellular framework.

4. Methods

4.1. Rainfall-Simulation Experiment

[37] To produce a rigorous test of the model, data are required on the spatial patterns of soil erosion under a range of detachment and transport conditions. This requirement was achieved by performing a controlled rainfall-simulation experiment on an artificial sediment plot.

[38] A plot was constructed that was 13.75 m long and 6.5 m wide. The left-hand half of the plot had a uniform gradient of 3°, whereas the right-side boundary was created to be at a gradient of 5°, resulting in a significant cross-slope on the left-hand side of the plot (Figure 3a). This surface was created so that the left-hand side of the plot was primarily subjected to raindrop impact while the right-hand side experienced both raindrop impact and flow detachment. A digital elevation model was obtained by surveying the plot on a 0.3 m grid using a total station. The material from which the plot was constructed comprised three sediment layers. The lowest layer of sand was used to fashion the shape of the plot and was compacted using a mechanical compactor followed by 30 min of rainfall at low intensity. On top of this layer, a 0.1 m-deep layer of sand was spread uniformly over the surface, compacted first by trampling, and then by low-intensity, simulated rain onto the surface. The top layer comprised a non-compacted, 0.05 m-deep layer of sand ($D_{50} = 0.16$ mm) (Figure 4).

[39] The top 5 mm of soil in a 0.3 m wide trench, the upslope boundary of which was located 5.7 m from the top of the plot (see Figure 3c), was replaced with a layer of ^{137}Cs-rich tracer soil by scraping off a layer of the topsoil across the width of the plot and adding the tracer soil into this shallow trench, and tamping it down so that it was flush with the pre-existing soil surface. The tracer soil had been pre-sieved so that its particle size distribution was a close match to that of the topsoil layer (Figure 4). Gutters, leading to an outflow midway across the plot, were installed along the downslope edge and sealed to the surface of the plot.

[40] A rainfall event lasting 20 min at a design rainfall intensity of 60 mm h^{-1} was simulated on the plot. A detailed investigation of the spatial pattern of the rainfall distribution (Figure 5) was undertaken, using buckets at 0.5 m spacing. This rainfall distribution was implemented in the model. Discharge and sediment loss were measured in the gutter by taking timed volumetric samples every 30 s throughout the experiments. A camera was mounted above the plot providing plan view, time-lapse photography of the development and evolution of the overland flow occurring on the plot. The images were processed to determine the change in area of inundation during the rainfall event.

[41] The spatial pattern of soil redistribution was determined by mapping the ^{137}Cs inventories at the end of the rainfall event. Using a scraper plate [*Loughran et al.*, 2002], 0.15 m by 0.3 m, soil-surface samples were collected on a 0.3 m grid from an area just upslope of the ^{137}Cs-rich layer of tracer soil to the downslope edge of the plot. ^{137}Cs concentration was measured using a gamma ray spectrometer with a Canberra Genie-2000 Spectroscopy System in these samples

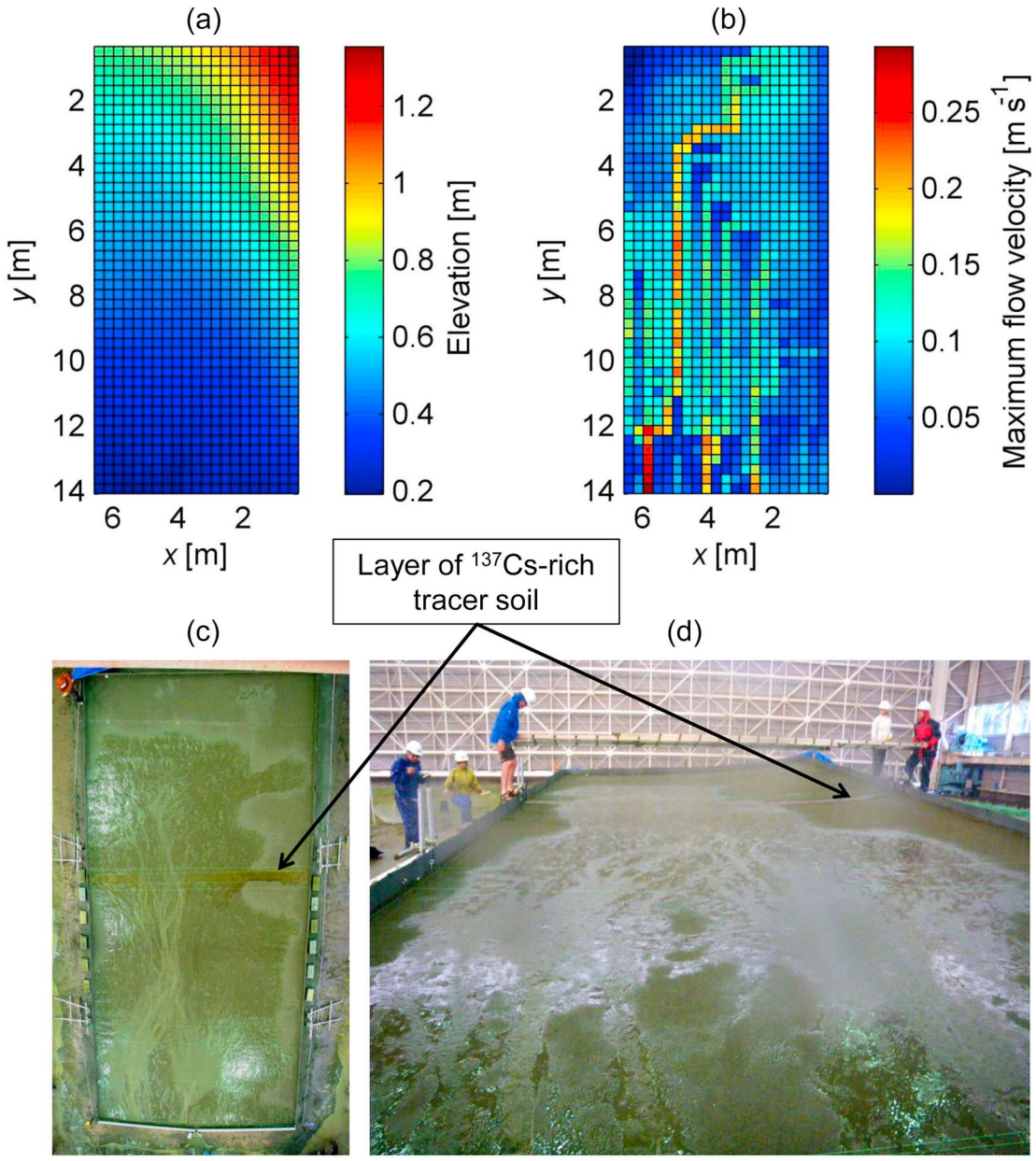

Figure 3. (a) Digital elevation model [m] represented within the cellular computational grid; (b) simulated maximum overland flow velocity [m s^{-1}]; (c) plan view of the spatial distribution of overland flow at the end of the storm event; and (d) a view from the downslope end of the plot revealing the formation of shallow rills.

and the runoff sediment. The MAHLERAN-MiC model used a cell size of 0.3 m to replicate the sampling grid.

4.2. Sensitivity to Number of Markers

[42] To produce a representative simulation of the redistribution of the ^{137}Cs-rich tracer soil, the minimum required number of markers in each cell was estimated. We assumed that a simulation using 6,000 markers in each cell – a total of 1,320,000 across the plot – would produce an unbiased estimate of the true, distribution of markers at the end of the rainfall event. The simulation was run 20 times, and the final distribution of markers for each run was recorded. This procedure was repeated for an ever-decreasing number of markers down to 10 markers per cell. For each number of markers, the final spatial distributions of markers from all the 20 replicates were compared to the 20 distributions produced using 6000 markers per cell. The comparison was made on a cell-by-cell basis using a two-sample t-test. The minimum required number of markers was defined as the number of markers in which more than 95% of the cells displayed no statistically significant difference (at the 5% significance level) to the distributions from the 20 simulations using 6000 markers. The results in Figure 6a reveal the minimum is 1200 markers per cell, representing a significant saving in computational time (Figure 6b). Above 1200

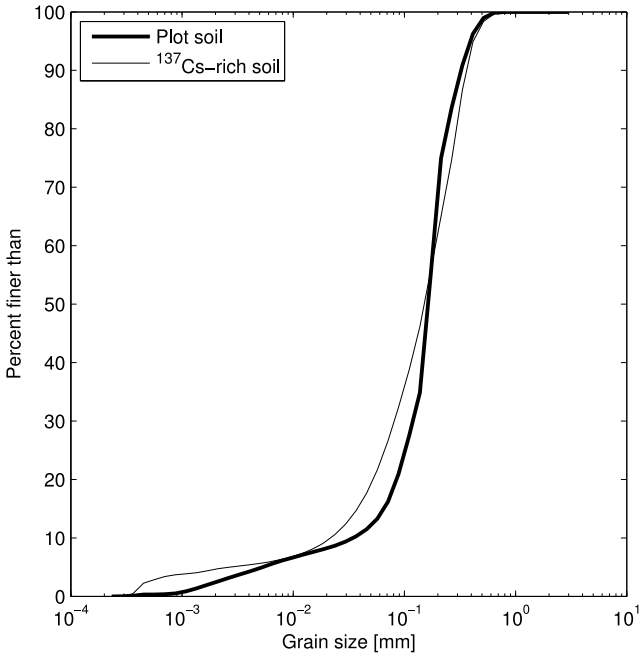

Figure 4. Grain-size distributions of plot soil and ^{137}Cs-rich tracer soil.

markers, computational accuracy is not sensitive to the number of markers used in the simulations. Similar results were found when a *Syrjala* [1996] test for differences in the spatial distribution was performed. These two results provide further evidence that 1200 markers per cell are sufficient. This was the number of markers used for the evaluation of model performance.

4.3. Simulation of Hydrology and Hydraulics

[43] We chose to calibrate the hydrology because our main interest lies in the erosion dynamics in the experiment. The construction of the slope allows us to assume relative uniformity of the hydrology parameters, and as noted above, the flow sub-model has been intensively tested.

[44] Calibration was carried out by maximizing the Nash-Sutcliffe efficiency statistic [*Nash and Sutcliffe*, 1970], and minimizing the normalized root-mean square error (NRMSE) for the modeled versus observed hydrograph. Calibration was carried out in three steps. First, the initial soil-moisture content was varied, then the values of final infiltration rate, and then finally the effective depth to the wetting front. This procedure provides a parsimonious and databased approach to calibration of the hydrograph.

[45] The Darcy-Weisbach friction factor $f[-]$ was parameterized using the approach developed by *Lawrence* [1997] in which f varies according to the degree of submergence of the surface roughness. This method has been shown by *Mügler et al.* [2011] to perform well for similar soil conditions as those found on the experimental plot. The strength of the approach is it provides spatial estimates of f, is physically based, and depends on the surface roughness properties (height and spatial coverage) and flow depth, and requires no calibration. The estimation of f is made according to whether the surface is partially, marginally or fully inundated, according to the definition within *Lawrence* [1997]. At partial inundation, when the flow depth is less than the characteristic roughness height h_c [m], the friction factor is estimated by:

$$f = \frac{8P_c C_D}{\pi} \min\left(\frac{\pi}{4}, \Lambda\right), \; 0 < \Lambda < 1 \tag{17}$$

where P_c is the proportion of the surface covered by the largest particles $[-]$, C_D is the drag coefficient of the surface roughness $[-]$, $\min(a, b)$ refers to the minimum value of either a or b and Λ is the inundation ratio $[-]$, defined as h_w/h_c. We take h_c to be equal to $D_{50}/2$ according to *Abrahams et al.* [1986], *Lawrence* [1997], and *Mügler et al.* [2011], and assume C_D to be equal to 1, as in the latter two studies. At marginal inundation, when the surface roughness is fully covered by the flow and h_w is of the same order of magnitude as h_c, frictional resistance is given by:

$$f = \frac{10}{\Lambda^2}, \; 1 \le \Lambda < 10. \tag{18}$$

At full inundation, where h_w is more than an order of magnitude greater than h_c, f is estimated by:

$$f = \frac{1}{(1.64 + 0.803 + \ln\Lambda)^2}, \; \Lambda \ge 10. \tag{19}$$

The outflow hydrograph is reproduced well with a Nash-Sutcliffe efficiency of 0.93 and NRMSE of 14.8% (Figure 7). The fluctuations in observed runoff may be a function of the turbulence characteristics of the flow not accounted for in the flow model. The simulated onset of runoff and the general shape of the rise in runoff match well with observation, which is important for reproducing the timing of flow detachment within the marker component of the model. The model

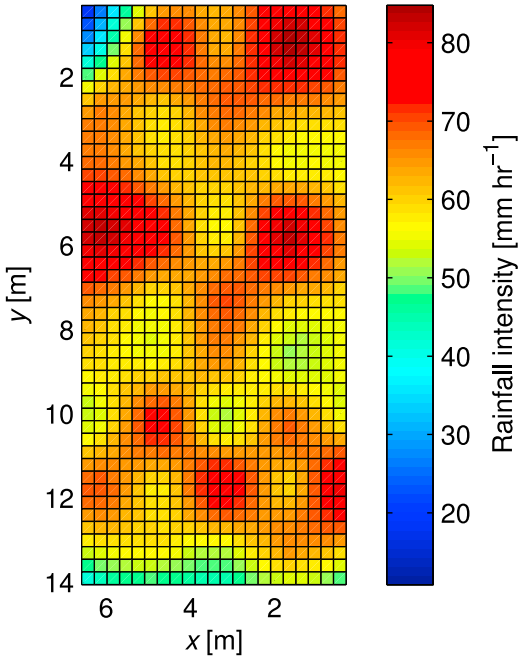

Figure 5. Measured rainfall intensity [mm h^{-1}] represented within the cellular framework.

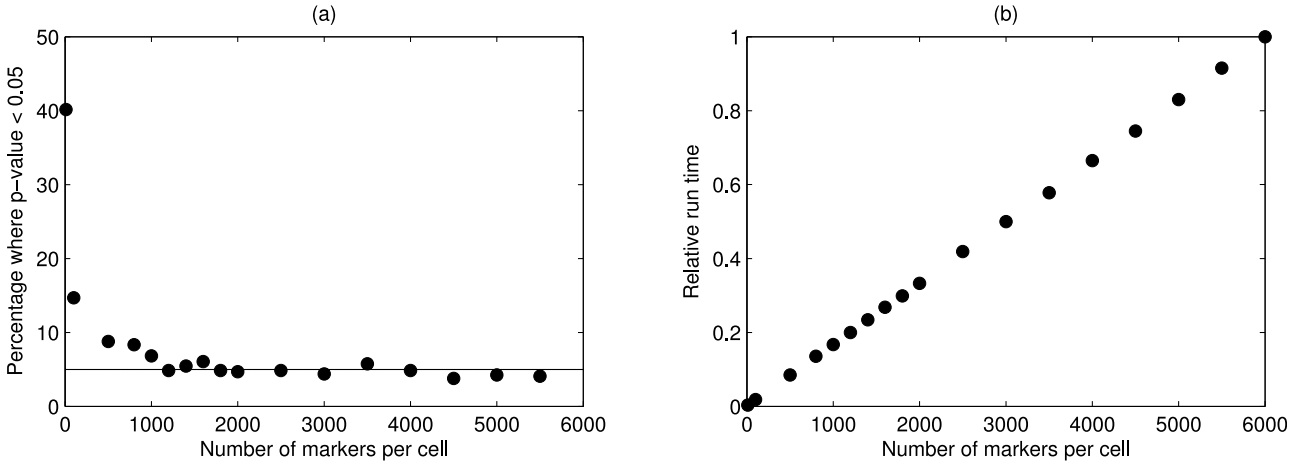

Figure 6. (a) Results of a two-sample t-test comparing the spatial distribution of markers using 6000 markers per cell to that using a lower number, showing the percentage of the cells in which there was a statistically significant difference (at the 5% significance level); (b) change in model run time relative to the run time using 6000 markers per cell.

simulates a total flow runoff of 580 L, which is close to the observed runoff of 534 L (a difference of 9%).

5. Model Evaluation

5.1. Hydraulics

[46] A comparison of the spatial distribution of overland flow inundation reveals that the cell-based model recreates the plot-scale structuring of the flow (see Figures 3b and 3c). The model is able to recreate the spatial distribution of inundation and its change with time (further seen in Figure 7b) and the concentration of the flow into longitudinal threads, particularly at the bottom of the plot, where shallow rills are formed (Figure 3d), and where the flow breaks the line of ^{137}Cs-rich tracer soil (Figure 3c). Thus, within the constraints of a calibrated and spatially discretized model, both the overall simulated hydrology and the key temporal and spatial aspects of the hydraulics can be considered to be good representations.

5.2. Spatial Patterns of Soil Erosion

[47] The marker component of the MAHLERAN-MiC model is used in an uncalibrated form to test the model. Figure 8 provides snapshots of the distribution of markers at four times during the storm event. The plots illustrate the change in spatial patterns of erosion as detachment and transport processes change from dominantly raindrop detachment and rain splash at the start of the event to dominantly flow detachment and transport.

[48] To compare the simulated results to the final spatial coverage of ^{137}Cs-rich tracer soil, the spatial coverage in each cell of the markers present on the plot was calculated. The spatial coverage in a given cell is given by the number of markers in the cell divided by the total number of markers present on the plot. This calculation was carried out for 20 simulations. Figure 9 compares the mean spatial coverage of the markers from the 20 replicates to the measured spatial

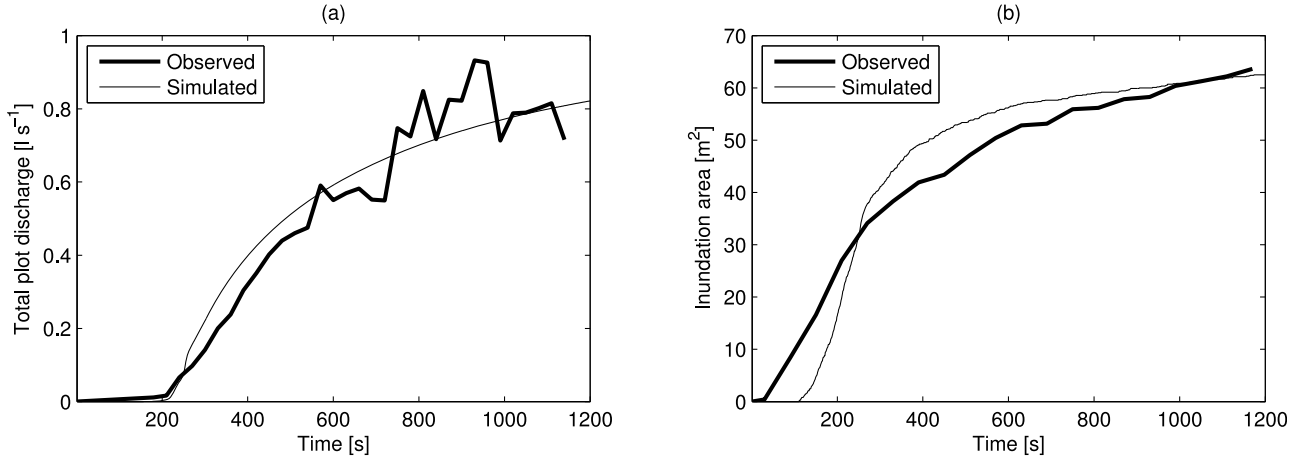

Figure 7. Comparison between observed and simulated (a) hydrograph and (b) flow inundation area. The observed inundation area was resolved from plan view photographs, an example of which is shown in Figure 3c.

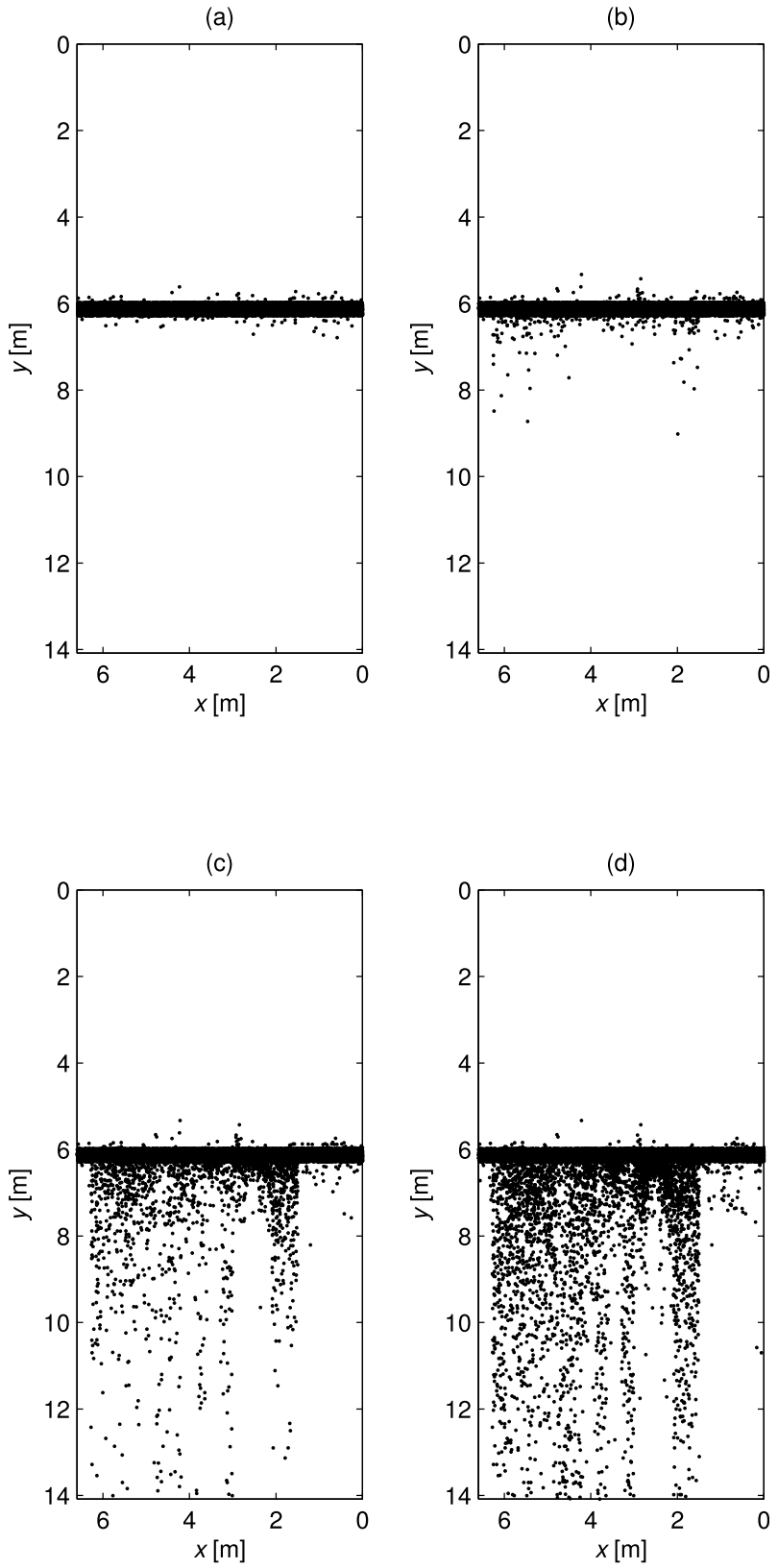

Figure 8. Distribution of markers at (a) 50, (b) 150, (c) 500 and (d) 1200 s during the rainfall event, illustrating how the movement responds to changes in sediment transport processes, from raindrop detachment and rain splash transport, to interrill erosion and to flow detachment and transport. The final distribution of markers is heavily influenced by the formation of threads of overland flow on the plot (see Figure 3b). Markers are exaggerated in size.

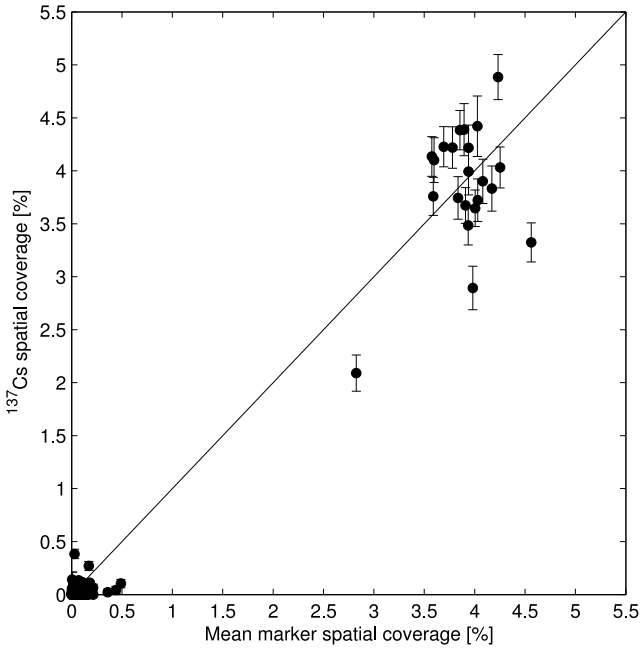

Figure 9. Comparison between the measured spatial coverage of ^{137}Cs-rich tracer soil and the spatial coverage of markers, on a cell-by-cell basis. The length of the error bars represents the range in spatial coverage of ^{137}Cs-rich tracer for each cell, accounting for the measurement error levels ($\pm$) in the ^{137}Cs inventories. The diagonal line is the 1:1 line.

coverage of ^{137}Cs-rich tracer soil, on a cell-by-cell basis. The spatial coverage of ^{137}Cs-rich tracer soil in each cell is given by the ^{137}Cs concentration in the cell divided by the total concentration present on the plot. Error bars in Figure 9 are included to account for the measurement error levels ($\pm$) in the ^{137}Cs inventories. The distribution of ^{137}Cs-rich tracer soil is reproduced well by the MiC model, with a Nash-Sutcliffe efficiency of 0.98 (0.97 and 0.97 with $\pm$ error levels included). The MiC model is able to reproduce areas where there is zero or little sediment deposition, as well as areas that have experienced significant deposition. The discrepancy between the measured and modeled results is not systematic, falling almost equally above and below the 1:1 line. Given that the marker component of the model is uncalibrated, this represents a promising result. The model also simulates an extremely close match between the time that markers are first transported off the end of the plot and the first time ^{137}Cs-rich tracer soil is detected in the gutter at the downslope edge of the slope (215 and 240 s, respectively).

6. Discussion

[49] Through the evaluation of the MAHLERAN-MiC we have shown that the heterogeneity of soil erosion can be represented without the need to consider the either the hillslope in terms of aggregate behavior, or representing the behavior of all grains as identical to the mean. The model structure allows a large difference between the range of possible sediment movement (which defines how much of the landscape can be modeled) and the particle size (which defines the scale at which the processes take place) [*Bithell and Macmillan*, 2007]. MAHLERAN-MiC tracks the source and sink of particles so it has the potential to be used to model the movement of contaminated sediment and understand sediment sources in rivers and reservoirs. Unlike many models of soil erosion which assume steady state erosion conditions (e.g., WEPP (Water Erosion Prediction Project) [*Laflen et al.*, 1991], KINEROS/KINEROS2 (KINematic runoff and EROSion model) [*Woolhiser et al.*, 1990], EUROSEM (European Soil Erosion Model) [*Morgan et al.*, 1998]), grain movement has been treated in a stochastic manner, better replicating the temporal dynamics of soil erosion. By incorporating the rainfall conditions, hydrology, hydraulics and individual grain movement within a single computational frame, the interactions between each can be examined explicitly. We are able to highlight the model limitations created by the lack of data for parameterization, as well as those in our understanding of soil erosion processes.

6.1. Model Limitations

[50] The MiC model was developed to produce a Lagrangian, stochastic and process-based description of soil erosion processes within a computationally efficient cellular framework. Our aim, where possible, was to parameterize the processes based on data sources that covered a wide range of slope, rainfall and overland-flow conditions. However, each of the processes was either necessarily oversimplified, parameterized using data from other fields of geomorphology or based on theoretical formulations from these fields. Here we consider the limitations of the marker component in replicating each of the detachment and transport processes. Those relating to the cell-based component of the model are discussed in detail in *Wainwright et al.* [2008c].

6.1.1. Raindrop Detachment and Rain Splash Transport

[51] It was not possible to treat fully the detachment process due to raindrop impact in a Lagrangian manner because of the paucity of data about the grain-scale dynamics. We are not aware of any study that has estimated the probability of detachment, even for simplified, single drop impacts. There is, however, a large body of literature that has measured the mass of sediment detached during rainfall events [e.g., *Savat*, 1981; *Erpul et al.*, 2004]. Thus, in order to simulate the probability of detachment for the range of sediment sizes, slope angles and rainfall intensities present on the experimental plot, it was necessary to draw upon this literature.

[52] A further limitation was that it was necessary to estimate the detachment/active layer depth. The fluvial literature suggests that the active layer reaches depths of up to $2D_{90}$ which varies according to grain size [*Wilcock et al.*, 1996; *Wilcock*, 1997; *DeVries*, 2002], shear stress/transport rate/stream power [*Haschenburger and Church*, 1998; *Wilcock et al.*, 1996; *Wilcock and McArdell*, 1997; *DeVries*, 2002] and flood history [*Haschenburger*, 2011]. No such information is available for raindrop or flow detachment on hillslopes. One would expect the depth to scale with grain size and time [*Wainwright et al.*, 2008a], reduce during a storm due to compaction, increase in size for more intense storms, and be shallower in interrill erosion. Our model takes no account of this likelihood.

[53] To provide a fully Lagrangian description of raindrop detachment and rain splash transport, a probability-density function of entrainment and how it varies with different conditions is required, as well as a joint probability-density

function of splash distance and direction (radial angle). We are aware of only one study that has considered splash from this standpoint. *Furbish et al.* [2007] assume that the radial redistribution of momentum of the deforming raindrop on impact approximates the radial distribution of splashed particles but do not account for the probability of detachment. Results from the splash experiments performed by *Furbish et al.* [2007] for dry beds showed that this was reasonable when Γ in equation (4) was given by $|u_s|/|u_n|$ through estimates of the fall velocity of a raindrop. However, the results also revealed that there is some scatter in the relationship between Γ and tan β, and the scatter is not consistent. Thus, if tan β is used to approximate Γ, as we have done, the resulting particle distribution will differ from the one estimated with the fall velocity of a raindrop, and therefore from the true distribution. This difference limits the application of the model because measurements would be required on the spatiotemporal distribution of drop velocity, or of drop diameter to estimate fall velocity. Its application may also be limited because an important component of the *Furbish et al.* [2007] model is untested with observations of individual, particle movement. *Furbish et al.* [2007] multiplied the probability-density function for splash distance by the function for radial angle to give the joint probability-density function, but Furbish et al. only used empirical observations to test the two constituent probability-density functions, not the joint probability-density function. By multiplying the two probability-density functions, they assumed that the two distributions of radial angle and splash distance were statistically independent. This assumption is unlikely because one would expect a higher likelihood of large splash distances in a given direction if more particles were splashed in that direction, which highlights the need to measure the grain-scale dynamics of the detachment and splash process if a fully Lagrangian description is to be provided. Testing this assumption is the subject of current work by the present authors (E. J. Long et al., manuscript in preparation, 2012).

6.1.2. Unconcentrated Flow Detachment

[54] To estimate the probability of detachment in unconcentrated flow conditions, it was necessary to use a theoretical formulation developed for the entrainment of gravel within a river [*Wu and Lin*, 2002]. We are not aware of any study that has quantified or formulated an expression for the probability of flow detachment on hillslopes.

[55] The extrapolation of theories from the fluvial literature to processes occurring on a hillslope, though commonplace, poses a number of potential problems, all of which also apply to the modeling of bed load and suspended load transport. First, there is no direct evidence that the mechanics of flow detachment and transport in rivers matches that found on a hillslope. A comparison is virtually impossible because there are so few observations on hillslopes. Second, the flow-inundation ratio under which transport occurs is usually higher for a river so the transport relationships developed for rivers may not scale to overland-flow conditions. Fluvial detachment rates are scaled by, among other things, bed shear velocity (or bed shear stress) and grain size. These parameters are used to extrapolate the transport relationships from the river to the hillslope. However, for a given bed shear velocity and grain size, the slope of a hillslope is likely to be greater than in a river, and the flow depth and inundation ratio will therefore be lower. To illustrate this, consider the following example. Take a hillslope with a typical slope of 0.2 [−] and a river with a slope of 0.005 [−], an identical bed shear velocity of 0.1 m s^{-1}, and composed of the same material (D_{50} = 0.0005 m). Given that $u_* = \sqrt{gh_w S}$, the flow depths h_w for the hillslope and river are 0.005 m and 0.2 m, respectively, so the inundation ratios are 20 and 815. This difference in inundation may be important when extrapolating the transport relationships from the river to the hillslope for the following reason. Within the fluvial literature there is strong evidence that the mean fluid shear stress at which sediment is entrained is inversely correlated to the inundation ratio [e.g., *Bathurst et al.*, 1983, 1987; *Shvidchenko and Pender*, 2000; *Mueller et al.*, 2005; *Parker et al.*, 2011] because the structure of the near-bed flow changes with this ratio [*Ashida and Bayazit*, 1973; *Graf*, 1991; *Lamb et al.*, 2008; *Cooper*, 2012]. Therefore the difference in the flow-inundation ratio between river and overland flows is likely to result in flow detachment rates on hillslopes being overestimated by fluvial transport equations. This difference may help explain the discrepancies that have been observed in modeled erosion rates for soil-erosion models that have used fluvial-transport relationships. For example, *Wainwright et al.* [2008b] found that MAHLERAN, which uses these relationships, consistently overestimated the sediment yield. Third, the use of bed shear velocity in fluvial studies in theoretical and empirical relationships, relies on the assumption of 2-D, steady, uniform flow, in which the vertical distribution of shear stress is linear and/or the velocity profile is logarithmic through the whole depth of flow. These conditions may not occur on hillslopes – we simply do not know. Fourthly, the transport relationships used in the model are all based on gravel-sized particles and extrapolated to finer particles. It is assumed the same detachment processes are applicable. However, differences in grain sizes are likely to produce differences in surface topography, such as packing, pivot angle, imbrication, exposed particle area, remote sheltering and roughness (grain and form) [*Wainwright et al.*, 1995]. These differences are likely to influence the near-bed flow field and the drag and lift (if any) forces exerted on the grain, which would result in significant differences in entrainment thresholds. Fifthly, transport distances may not scale from a river to a hillslope because of differences in flow conditions. Returning to the example of the two flows on a hillslope and a river with a bed shear velocity of 0.1 m s^{-1}, and the same surface grain size but vastly different inundation ratios, it follows from equation (19) that the friction factor will be higher for the hillslope and therefore the flow velocity will be slower. Assuming that transport distance is correlated to flow velocity, such as through equation (7) for interrill flow transport, it suggests that transport distance will be overestimated by fluvial models (as found by the comparison of the results of *Parsons et al.* [1998] and *Hassan et al.* [1992], in *Wainwright et al.* [2008a]). Finally, the differences in hydraulics discussed above may be further enhanced by the impact of raindrops on overland flow, because the effects of raindrops are usually ignored in fluvial studies. Studies within oceanic environments suggest this difference may be important. Observations have shown that rainfall can attenuate sea-wave height through generating turbulence in the upper column of the water surface [e.g., *Nystuen*, 1990; *Tsimplis*, 1992] and can increase surface roughness [e.g.,

Moore et al., 1979; *Craeye et al.*, 1997]. Thus, it is plausible that in shallow overland flows the exchange of momentum between a raindrop and the surrounding flow might influence its flow structure and resulting detachment rates (either through raindrop or flow detachment). Overall, the six potential problems discussed above show that it is necessary to evaluate the extent to which an extrapolation of transport relationships from river flows to hillslopes is reasonable.

6.1.3. Interrill Flow Transport

[56] The basis for the parameterization of particle travel distance and velocity for interrill flow transport is limited. *Parsons et al.* [1998] used a range of relatively coarse particles to determine distance and velocity because of experimental limitations. It has therefore been necessary to extrapolate the relationships beyond the data upon which they were originally based. Given the nonlinear nature of the relationships, small discrepancies in the manner in which the variables control the travel distance and velocity of finer particles may result in errors arising from the extrapolation of results for coarse grains. For example, *Wainwright et al.* [2008a] showed that the level of error in predicting travel distance and velocity for finer particles was sensitive to the form of the equation used in the extrapolation. Furthermore the use of overland flow energy within the transport relationships assumes, implicitly, the presence of steady and uniform flow. The duration of motion for particles in interrill flow transport was calculated from estimates of travel distance and velocity drawn from two independent exponential probability-density functions. This assumption of statistical independence is unlikely to hold, because particles with a higher velocity will tend to travel larger distances.

[57] Particle travel in interrill flow has been explored experimentally by *Kinnell* [1991; 2001] for finer particles of 0.11–0.9 mm. He calculated mass-weighted average travel distances for coal and sand based on spatially distributed measurements of transported mass. As we discussed for raindrop detachment, mass-weighted estimates do not provide a means by which to treat the transport processes in interrrill conditions in a Lagrangian manner. Little is known on the shape of the distribution function for travel distance in interrill flow for fine particles, and less still on travel velocity. For example, *Kinnell* [2009] produced a mechanistic model of the downstream movement of particle transport in interrill conditions based, partially, on the results in *Kinnell* [2001]. He makes the assumption that particles in interrill flow move with a velocity equal to 80% of the flow velocity when saltating, and move at the velocity of the flow when in suspension. This assumption remains untested.

6.1.4. Bed Load Detachment and Transport

[58] The statistical model of bed load detachment and transport was based on a limited set of empirical observations. For example, the shapes of the probability-density functions for the motion duration and distance were deduced from measurements taken for one grain size and one flow condition. Although the median motion duration and travel distance were scaled according to grain size and excess shear stress, the same distribution shape was assumed to apply across the range of conditions present on the experimental plot. Also the probability-density function of rest duration was based on just one data set and from one sediment mixture. As such, the estimation of motion duration and distance, and rest duration, suffer from the same extrapolation issues as identified for interrill flow transport.

[59] We assumed that the distributions for motion and rest duration, and transport distance were independent, based partially on the results of *Ancey et al.* [2006], and because we were examining soil movement during a single storm event for a relatively homogeneous fine-grain bed. At present there is no means by which to test this assumption for hillslopes. However, it would be expected that 'memory' would be important. A grain is likely to come to rest in a more sheltered position than its original location so a flow event with larger momentum will be required to remobilize the grain, increasing its subsequent resting duration and travel distance. Furthermore a particle that has traveled further may well be deposited in a more stable position than those that have traveled a shorter distance. For example, *Ferguson et al.* [2002] have demonstrated an apparent deceleration of tagged movement of fluvial gravel through a succession of floods, which may relate to the structure of bed material. *Wainwright and Thornes* [1991] and *Parsons et al.* [1993] make similar observations for particles moving on hillslopes following multiple storm events. Furthermore in rivers, sub-threshold flows [e.g., *Paphitis and Collins*, 2005] and above-threshold flows [e.g., *Hassan et al.*, 2006] have been shown to increase detachment thresholds for sands and gravels. If memory or past events are also found to be important for the movement of soil on hillslopes, bed load detachment and transport will need to be simulated as an nth-order or semi-Markov process [*Cox and Miller*, 1965], requiring observations of individual grain motion over large spatiotemporal scales and following multiple storm events.

6.1.5. Suspended Detachment and Transport

[60] There is an almost complete lack of information of the flow detachment and transport process of grains suspended in overland flow, despite many assuming that all transport occurs in suspension [see *Wainwright et al.*, 2008a]. It was necessary to modify a process-based model from aeolian geomorphology to determine the transport distance and velocity of grains in suspension. Although, conceptually, there should be no problem with this extrapolation, in practice there are likely to be some differences. Also the flow and turbulence model was based on measurements made for open channel flows, and is limited by the assumption of 2-D, uniform flow, as discussed above. The influence of moving particles on the turbulence structure (damping effects), shown to be important in open channel flows [e.g., *Vanoni and Nomicos*, 1960, *Gust and Southard*, 1983; *Campbell et al.*, 2005], was also ignored.

6.1.6. Model Structure

[61] In terms of the overall structure of the marker component of the model, there are a number of issues that remain to be resolved, all of which also require greater understanding of the detachment and transport processes. First, we do not know the exact conditions under which the different detachment and transport conditions occur, even in a probabilistic sense. For fluvial sediment transport, *Einstein* [1950, p. 7] noted "the assumption of a sharp limit between bed load and wash [suspended] load must be understood as a convenient simplification of a basically complex gradual transition. Virtually nothing is known about this transition today." This situation is certainly still the case for erosion on hillslopes, and also exists in the fluvial literature. For example, *van Rijn*

[1984] estimates a (deterministic) threshold criterion for bed load and suspended load transport, but based on observations in simplified, steady, uniform flows in a hydraulic flume. *Kinnell* [2005] presents a conceptual model for the different detachment and transport conditions, using raindrop kinetic energy and overland flow stream power as thresholds between the different processes. Empirical observations have yet to provide numbers for these thresholds. Second, the MiC model assumes that the markers are always present on the surface, can exist in any spatial location, regardless of the location of others, are always available for detachment and do not become buried. As *Hairsine and Rose* [1992a, 1992b] noted, the probability of detachment is dependent upon whether the particle resides in the deposited layer or in the unshielded original soil layer. Therefore more observations are required on the vertical dynamics of soil erosion (see discussion above on the active layer) because it controls the rate of detachment. Third, the MiC model treats transport as occurring through a discrete process. Once detached the markers are not acted upon by different transport processes and do not interact, whereas in reality some will collide or impact upon others on the bed surface, modifying the transport distance and entrainment threshold of a marker. Fourthly, in the model, only the rainfall and flow conditions in the cell at the point of detachment determine the transport distance and velocity of a marker, rather than being modified during its trajectory. Fifthly, markers are treated as discrete entities; they are not influenced by the transport status of others. Evidence from the fluvial literature suggests this is not appropriate. Bursts of movement, or sediment pluses [e.g., *Drake et al.*, 1988; *Cudden and Hoey*, 2003], have been observed to occur because the movement of individual grains exposes others to the flow. Also, evidence from bed load-transport studies in rivers shows that size fractions in sediment mixtures have different entrainment thresholds from those in a uniform size distribution, particularly when sand is present within a coarser mixture [e.g., *Wilcock et al.*, 2001]. Sixthly, in reality the parameterizations of the detachment processes are likely to be more complex functions of factors such as surface topography and turbulence length scales. Finally, MiC is by necessity a highly parameterized model so the model is constrained by the empirical base upon which the parameterization rests. Its performance outside the parameterized conditions is uncertain, especially given that the parameterized conditions are already wildly extrapolated in some cases. Highly parameterized models will remain until the soil erosion community follows through the implications of different hydraulic and sediment transport theory used in soil erosion modeling, from the assumption of steady, uniform, 2-D flows to the assumption that fluvial theories of transport hold on hillslopes.

7. Conclusions

[62] We have developed a new type of soil-erosion model, a marker-in-cell model, which simulates the redistribution of soil during rainfall events. The model is a hybrid of cell- and particle-based techniques and allows, for the first time, two-dimensional spatial patterns of individual particle movement on a hillslope to be simulated within a computationally efficient framework. The model simulates all the processes of detachment and transport and allows erosion to be treated in a fully stochastic manner. The spatial pattern of erosion is determined directly by the movement of the individual sediment particles rather than through mathematical expressions that represent the average behavior of particles.

[63] We tested the MiC model using data collected from a plot-scale, rainfall-simulation experiment. We measured the redistribution of ^{137}Cs-rich tracer soil to resolve the spatial patterns of erosion caused by a single, high-intensity, rainfall event. The model was able to recreate the key temporal and spatial aspects of the hydrology and hydraulics occurring on the plot, as well as the spatial redistribution of ^{137}Cs-rich tracer soil. It revealed that the MiC model is able to simulate plot-scale erosion from the explicit simulation of grain-scale, sediment processes. Since the model is able to track the sources and sinks of particles, it has the potential to be used to model the movement of contaminated sediment and understand sediment sources in rivers and reservoirs.

[64] The development of the model has provided a key feedback to the understanding of how to investigate soil erosion processes. The lack of empirical underpinnings of the different model components has highlighted where data limitations lie. There is a need to understand the spatiotemporal dynamics of soil erosion processes at the grain-scale, and preferably with simultaneous measurements of rainfall and flow dynamics so that a process-based understanding of detachment and transport can be sought. Further work, which measures these spatiotemporal dynamics in conjunction with iterative model development, is required.

[65] **Acknowledgments.** This research was supported by NERC grant NE/H006176/1. Some of this work was conducted while Parsons was in receipt of a visiting professorship at Tsukuba University, Japan. We thank the Associate Editor and two anonymous reviewers for their constructive comments.

References

Abrahams, A. D., A. J. Parsons, and S. H. Luk (1986), Resistance to overland-flow on desert hillslopes, *J. Hydrol.*, *88*(3–4), 343–363, doi:10.1016/0022-1694(86)90099-5.

Al-Durrah, M. M., and J. M. Bradford (1982), Parameters for describing soil detachment due to single water-drop impact, *Soil Sci. Soc. Am. J.*, *46*(4), 836–840, doi:10.2136/sssaj1982.03615995004600040034x.

Ancey, C. (2010), Stochastic modeling in sediment dynamics: Exner equation for planar bed incipient bed load transport conditions, *J. Geophys. Res.*, *115*, F00A11, doi:10.1029/2009JF001260.

Ancey, C., T. Bohm, M. Jodeau, and P. Frey (2006), Statistical description of sediment transport experiments, *Phys. Rev. E*, *74*(1), 011302, doi:10.1103/PhysRevE.74.011302.

Anderson, R. S. (1987), Eolian sediment transport as a stochastic-process: The effects of a fluctuating wind on particle trajectories, *J. Geol.*, *95*(4), 497–512, doi:10.1086/629145.

Antonia, R., and P. A. Krogstad (2001), Turbulence structure in boundary layers over different types of surface roughness, *Fluid Dyn. Res.*, *28*(2), 139–157, doi:10.1016/S0169-5983(00)00025-3.

Ashida, K., and M. Bayazit (1973), Initiation of motion and roughness of flows in steep channels, paper presented at 15th Congress, Int. Assoc. Hydraul. Res., Istanbul, Turkey.

Balachandar, R., and V. C. Patel (2002), Rough wall boundary layer on plates in open channels, *J. Hydraul. Eng.*, *128*(10), 947–951, doi:10.1061/(ASCE)0733-9429(2002)128:10(947).

Bathurst, J. C., W. H. Graf, and H. H. Cao (1983), Initiation of sediment transport in steep channels with coarse bed material, in *Mechanics of Sediment Transport*, edited by B. M. Sumer and A. Muller, pp. 207–213, A. A. Balkema, Rotterdam, Netherlands.

Bathurst, J. C., W. H. Graf, and H. H. Cao (1987), Bed load discharge equations for steep mountain rivers, in *Sediment Transport in Gravel-Bed Rivers*, edited by C. R. Thorne, J. C. Bathurst, and R. D. Hey, pp. 453–477, John Wiley, New York.

Bergstrom, D. J., M. F. Tachie, and R. Balachandar (2001), Application of power laws to low Reynolds number boundary layers on smooth and rough surfaces, *Phys. Fluids*, *13*(11), 3277–3284, doi:10.1063/1.1410383.

Beven, K. (2001), On hypothesis testing in hydrology, *Hydrol. Processes*, *15*(9), 1655–1657, doi:10.1002/hyp.436.

Bigillon, F., Y. Nino, and M. H. Garcia (2006), Measurements of turbulence characteristics in an open-channel flow over a transitionally rough bed using particle image velocimetry, *Exp. Fluids*, *41*(6), 857–867, doi:10.1007/s00348-006-0201-2.

Bithell, M., and W. D. Macmillan (2007), Escape from the cell: Spatially explicit modelling with and without grids, *Ecol. Modell.*, *200*(1–2), 59–78, doi:10.1016/j.ecolmodel.2006.07.031.

Blöschl, G., R. B. Grayson, and M. Sivapalan (1995), On the Representative Elementary Area (REA) concept and its utility for distributed rainfall-runoff modeling, *Hydrol. Processes*, *9*(3–4), 313–330, doi:10.1002/hyp.3360090307.

Brackbill, J. U., and H. M. Ruppel (1986), FLIP: A method for adaptively zoned, particle-in-cell calculations of fluid-flows in two dimensions, *J. Comput. Phys.*, *65*(2), 314–343, doi:10.1016/0021-9991(86)90211-1.

Bradford, J. M., P. A. Remley, J. E. Ferris, and J. B. Santini (1986), Effect of soil surface sealing on splash from a single waterdrop, *Soil Sci. Soc. Am. J.*, *50*(6), 1547–1552, doi:10.2136/sssaj1986.03615995005000060033x.

Bradford, J. M., J. E. Ferris, and P. A. Remley (1987a), Interrill soil-erosion processes: I. Effect of surface sealing on infiltration, runoff, and soil splash detachment, *Soil Sci. Soc. Am. J.*, *51*(6), 1566–1571, doi:10.2136/sssaj1987.03615995005100060029x.

Bradford, J. M., J. E. Ferris, and P. A. Remley (1987b), Interrill soil-erosion processes: II. Relationship of splash detachment to soil properties, *Soil Sci. Soc. Am. J.*, *51*(6), 1571–1575, doi:10.2136/sssaj1987.03615995005100060030x.

Butler, T. D., I. Henins, F. C. Jahoda, J. Marshall, and R. L. Morse (1969), Coaxial snowplow discharge, *Phys. Fluids*, *12*(9), 1904–1916, doi:10.1063/1.1692758.

Calantoni, J., K. T. Holland, and T. G. Drake (2004), Modelling sheet-flow sediment transport in wave-bottom boundary layers using discrete-element modelling, *Philos. Trans. R. Soc. London A*, *362*(1822), 1987–2001.

Campbell, L., I. McEwan, V. Nikora, D. Pokrajac, M. Gallagher, and C. Manes (2005), Bed-load effects on hydrodynamics of rough-bed open-channel flows, *J. Hydraul. Eng.*, *131*(7), 576–585, doi:10.1061/(ASCE)0733-9429(2005)131:7(576).

Cooper, J. R. (2012), Does flow variance affect bedload flux when the bed is dominated by grain roughness?, *Geomorphology*, *141*, 160–169, doi:10.1016/j.geomorph.2011.1012.1039.

Cox, D. R. (1962), *Renewal Theory*, Methuen, London.

Cox, D. R., and H. D. Miller (1965), *The Theory of Stochastic Processes*, Metheun, London.

Craeye, C., P. W. Sobieski, and L. F. Bliven (1997), Scattering by artificial wind and rain roughened water surfaces at oblique incidences, *Int. J. Remote Sens.*, *18*(10), 2241–2246, doi:10.1080/014311697217864.

Cudden, J. R., and T. B. Hoey (2003), The causes of bedload pulses in a gravel channel: The implications of bedload grain-size distributions, *Earth Surf. Processes Landforms*, *28*(13), 1411–1428, doi:10.1002/esp.521.

DeVries, P. (2002), Bedload layer thickness and disturbance depth in gravel bed streams, *J. Hydraul. Eng.*, *128*(11), 983–991, doi:10.1061/(ASCE)0733-9429(2002)128:11(983).

Dietrich, W. E., and P. Whiting (1989), Boundary shear stress and sediment transport in river meanders of sand and gravel, in *River Meandering*, *Water Resour. Monogr. Ser*, vol. 12, edited by S. Ikeda and G. Parker, pp. 1–50, AGU, Washington, D. C.

Drake, T. G., R. L. Shreve, W. E. Dietrich, P. J. Whiting, and L. B. Leopold (1988), Bedload transport of fine gravel observed by motion-picture photography, *J. Fluid Mech.*, *192*, 193–217, doi:10.1017/S0022112088001831.

Drewry, J. J., R. J. Paton, and R. M. Monaghan (2004), Soil compaction and recovery cycle on a Southland dairy farm: Implications for soil monitoring, *Aust. J. Soil Res.*, *42*(7), 851–856, doi:10.1071/SR03169.

Durrett, R., and S. Levin (1994), The importance of being discrete (and spatial), *Theor. Popul. Biol.*, *46*(3), 363–394, doi:10.1006/tpbi.1994.1032.

Einstein, H. A. (1937), *Der geschiebetrieb als wahrscheinlichkeitsproblem (Bedload Transport as a Probability Problem)*, Verlag Rascher, Zürich. [English translation in *Sedimentation*, edited by H. W. Shen, H. W., pp. C1971–C1105, Water Resour. Publ., Fort Collins, Colo, 1972.]

Einstein, H. A. (1942), Formulas for the transport of bed sediment, *Trans. Am. Soc. Civ. Eng.*, *107*, 561–574.

Einstein, H. A. (1950), The bed-load function for sediment transportation in open channel flows, *Tech. Bull. 1026*, U.S. Dep. of Agric., Soil Conserv. Serv., Washington, D. C.

Erpul, G., L. D. Norton, and D. Gabriels (2004), Splash-saltation trajectories of soil particles under wind-driven rain, *Geomorphology*, *59*(1–4), 31–42, doi:10.1016/j.geomorph.2003.09.003.

Farres, P. J. (1987), The dynamics of rainsplash erosion and the role of soil aggregate stability, *Catena*, *14*(1–3), 119–130, doi:10.1016/S0341-8162(87)80009-7.

Ferguson, R. I., D. J. Bloomer, T. B. Hoey, and A. Werritty (2002), Mobility of river tracer pebbles over different timescales, *Water Resour. Res.*, *38*(5), 1045, doi:10.1029/2001WR000254.

Furbish, D. J., and P. K. Haff (2010), From divots to swales: Hillslope sediment transport across divers length scales, *J. Geophys. Res.*, *115*, F03001, doi:10.1029/2009JF001576.

Furbish, D. J., K. K. Hamner, M. Schmeeckle, M. N. Borosund, and S. M. Mudd (2007), Rain splash of dry sand revealed by high-speed imaging and sticky paper splash targets, *J. Geophys. Res.*, *112*, F01001, doi:10.1029/2006JF000498.

Graf, W. H. (1991), Flow resistance over a gravel bed: Its consequences on initial sediment movement, in *Fluvial Hydraulics in Mountain Regions*, edited by A. Armanini and G. Di Silvio, pp. 15–32, Springer, Berlin, doi:10.1007/BFb0011179.

Grass, A. J. (1970), Initial instability of fine bed sand, *J. Hydraul. Div. Am. Soc. Civ. Eng.*, *96*, 619–632.

Gust, G., and J. B. Southard (1983), Effects of weak bed-load on the universal law of the wall, *J. Geophys. Res.*, *88*(C10), 5939–5952, doi:10.1029/JC088iC10p05939.

Guy, H. P., D. B. Simons, and E. V. Richardson (1966), Summary of alluvial channel data from flume environments, 1956–1961, *U.S. Geol. Surv. Prof. Pap.*, *462-I*, 96 pp.

Hairsine, P. B., and C. W. Rose (1992a), Modeling water erosion due to overland-flow using physical principles: 1. Sheet flow, *Water Resour. Res.*, *28*(1), 237–243, doi:10.1029/91WR02380.

Hairsine, P. B., and C. W. Rose (1992b), Modeling water erosion due to overland-flow using physical principles: 2. Rill flow, *Water Resour. Res.*, *28*(1), 245–250, doi:10.1029/91WR02381.

Harlow, F. H. (1957), Hydrodynamics problem involving large fluid distortions, *J. ACM*, *4*(2), 137–142, doi:10.1145/320868.320871.

Haschenburger, J. K. (2011), Vertical mixing of gravel over a long flood series, *Earth Surf. Processes Landforms*, *36*(8), 1044–1058, doi:10.1002/esp.2130.

Haschenburger, J. K., and M. Church (1998), Bed material transport estimated from the virtual velocity of sediment, *Earth Surf. Processes Landforms*, *23*(9), 791–808, doi:10.1002/(SICI)1096-9837(199809)23:9<791::AID-ESP888>3.0.CO;2-X.

Hassan, M. A., M. Church, and P. J. Ashworth (1992), Virtual rate and mean distance of travel of individual clasts in gravel-bed channels, *Earth Surf. Processes Landforms*, *17*(6), 617–627, doi:10.1002/esp.3290170607.

Hassan, M. A., R. Egozi, and G. Parker (2006), Experiments on the effect of hydrograph characteristics on vertical grain sorting in gravel bed rivers, *Water Resour. Res.*, *42*, W09408, doi:10.1029/2005WR004707.

Heays, K. G., H. Friedrich, and B. W. Melville (2010), Advanced particle tracking for sediment movement on river beds: A laboratory study, paper presented at 17th Australasian Fluid Mechanics Conference, Univ. of Auckland, Auckland, New Zealand, 5–9 Dec.

Heng, B. C. P., G. C. Sander, A. Armstrong, J. N. Quinton, J. H. Chandler, and C. F. Scott (2011), Modeling the dynamics of soil erosion and size-selective sediment transport over nonuniform topography in flume-scale experiments, *Water Resour. Res.*, *47*, W02513, doi:10.1029/2010WR009375.

Hubbell, D., and W. Sayre (1964), Sand transport studies with radioactive tracers, *J. Hydraul. Div. Am. Soc. Civ. Eng.*, *90*, 39–68.

Johnson, B. E., P. Y. Julien, D. K. Molnar, and C. C. Watson (2000), The two-dimensional upland erosion model CASC2D-SED, *J. Am. Water Resour. Assoc.*, *36*(1), 31–42, doi:10.1111/j.1752-1688.2000.tb04246.x.

Kang, L. Q. (2012), Discrete particle model of aeolian sand transport: Comparison of 2D and 2.5D simulations, *Geomorphology*, *139–140*, 536–544, doi:10.1016/j.geomorph.2011.12.005.

Kang, L. Q., L. J. Guo, and D. Y. Liu (2008), Reconstructing the vertical distribution of the aeolian saltation mass flux based on the probability distribution of lift-off velocity, *Geomorphology*, *96*(1–2), 1–15, doi:10.1016/j.geomorph.2007.07.005.

Kinnell, P. I. A. (1974), Splash erosion: Some observations on the splash-cup technique, *Soil Sci. Soc. Am. Proc.*, *38*, 657–660.

Kinnell, P. I. A. (1990), The mechanics of raindrop-induced flow transport, *Aust. J. Soil Res.*, *28*(4), 497–516, doi:10.1071/SR9900497.

Kinnell, P. I. A. (1991), The effect of flow depth on sediment transport induced by raindrops impacting shallow flows, *Trans. ASAE*, *34*, 161–168.

Kinnell, P. I. A. (1993), Sediment concentrations resulting from flow depth/drop size interactions in shallow overland flow, *Trans. ASAE*, *36*(4), 1099–1103.

Kinnell, P. I. A. (2001), Particle travel distances and bed and sediment compositions associated with rain-impacted flows, *Earth Surf. Processes Landforms*, *26*(7), 749–758, doi:10.1002/esp.221.

Kinnell, P. I. A. (2005), Raindrop-impact-induced erosion processes and prediction: A review, *Hydrol. Processes*, *19*(14), 2815–2844, doi:10.1002/hyp.5788.

Kinnell, P. I. A. (2009), The influence of raindrop induced saltation on particle size distributions in sediment discharged by rain-impacted flow on planar surfaces, *Catena*, *78*(1), 2–11, doi:10.1016/j.catena.2009.01.008.

Kinnell, P. I. A. (2012), Raindrop-induced saltation and the enrichment of sediment discharged from sheet and interrill erosion areas, *Hydrol. Processes*, *26*(10), 1449–1456, doi:10.1002/hyp.8270.

Kironoto, B. A., and W. H. Graf (1994), Turbulence characteristics in rough uniform open-channel flow, *Proc. ICE Water Mar. Eng.*, *106*(4), 333–344.

Laflen, J. M., L. J. Lane, and G. R. Foster (1991), WEPP: A new generation of erosion prediction technology, *J. Soil Water Conserv.*, *46*(1), 34–38.

Lajeunesse, E., L. Malverti, and F. Charru (2010), Bed load transport in turbulent flow at the grain scale: Experiments and modeling, *J. Geophys. Res.*, *115*, F04001, doi:10.1029/2009JF001628.

Lamb, M. P., W. E. Dietrich, and J. G. Venditti (2008), Is the critical Shields stress for incipient sediment motion dependent on channel-bed slope?, *J. Geophys. Res.*, *113*, F02008, doi:10.1029/2007JF000831.

Lange, R. (1978), ADPIC: A three-dimensional particle-in-cell model for the dispersal of atmospheric pollutants and its comparison to regional tracer studies, *J. Appl. Meteorol.*, *17*, 320–329, doi:10.1175/1520-0450(1978)017<0320:ATDPIC>2.0.CO;2.

Lawrence, D. S. L. (1997), Macroscale surface roughness and frictional resistance in overland flow, *Earth Surf. Processes Landforms*, *22*(4), 365–382, doi:10.1002/(SICI)1096-9837(199704)22:4<365::AID-ESP693>3.0.CO;2–6.

Lisle, I. G., C. W. Rose, W. L. Hogarth, P. B. Hairsine, G. C. Sander, and J. Y. Parlange (1998), Stochastic sediment transport in soil erosion, *J. Hydrol.*, *204*(1–4), 217–230, doi:10.1016/S0022-1694(97)00123-6.

Loughran, R. J., P. J. Wallbrink, D. E. Walling, and P. G. Appleby (2002), Sampling methods, in *Handbook for the Assessment of Soil Erosion and Sedimentation Using Environmental Radionuclides*, edited by F. Zapata, pp. 41–57, Kluwer, Boston, Mass., doi:10.1007/0-306-48054-9_3.

McEwan, I., and J. Heald (2001), Discrete particle modeling of entrainment from flat uniformly sized sediment beds, *J. Hydraul. Eng.*, *127*(7), 588–597, doi:10.1061/(ASCE)0733-9429(2001)127:7(588).

Moore, R. K., Y. S. Yu, A. K. Fung, D. Kaneko, G. J. Dome, and R. E. Werp (1979), Preliminary study of rain effects on radar scattering from water surfaces, *IEEE J. Oceanic Eng.*, *4*(1), 31–32, doi:10.1109/JOE.1979.1145408.

Morgan, R. P. C., J. N. Quinton, R. E. Smith, G. Govers, J. W. A. Poesen, K. Auerswald, G. Chisci, D. Torri, and M. E. Styczen (1998), The European Soil Erosion Model (EUROSEM): A dynamic approach for predicting sediment transport from fields and small catchments, *Earth Surf. Processes Landforms*, *23*(6), 527–544, doi:10.1002/(SICI)1096-9837(199806)23:6<527::AID-ESP868>3.0.CO;2–5.

Mosley, M. P. (1973), Rainsplash and the convexity of badland divides, *Z. Geomorphol.*, *18*, Suppl., 10–25.

Mueller, E. R., J. Pitlick, and J. M. Nelson (2005), Variation in the reference shields stress for bed load transport in gravel-bed streams and rivers, *Water Resour. Res.*, *41*, W04006, doi:10.1029/2004WR003692.

Mügler, C., O. Planchon, J. Patin, S. Weill, N. Silvera, P. Richard, and E. Mouche (2011), Comparison of roughness models to simulate overland flow and tracer transport experiments under simulated rainfall at plot scale, *J. Hydrol.*, *402*(1–2), 25–40, doi:10.1016/j.jhydrol.2011.02.032.

Müller, E. N., J. Wainwright, and A. J. Parsons (2007), The stability of vegetation boundaries and the propagation of desertification in the American Southwest: A modelling approach, *Ecol. Modell.*, *208*(2–4), 91–101, doi:10.1016/j.ecolmodel.2007.04.010.

Nash, J. E., and J. V. Sutcliffe (1970), River flow forecasting through conceptual models. Part I: A discussion of principles, *J. Hydrol.*, *10*, 282–290, doi:10.1016/0022-1694(70)90255-6.

Nearing, M. A., and J. M. Bradford (1985), Single waterdrop splash detachment and mechanical properties of soils, *Soil Sci. Soc. Am. J.*, *49*(3), 547–552, doi:10.2136/sssaj1985.03615995004900030003x.

Nezu, I. (1977), Turbulent structure in open-channel flows, PhD thesis, Kyoto Univ., Kyoto, Japan.

Nezu, I., and H. Nakagawa (1993), *Turbulence in Open Channel Flows*, A. A. Balkema, Rotterdam, Netherlands.

Nystuen, J. A. (1990), A note on the attenuation of surface gravity-waves by rainfall, *J. Geophys. Res.*, *95*(C10), 18,353–18,355, doi:10.1029/JC095iC10p18353.

Paintal, A. (1971), A stochastic model of bed load transport, *J. Hydraul. Res.*, *9*, 527–554, doi:10.1080/00221687109500371.

Papanicolaou, A. N., P. Diplas, N. Evaggelopoulos, and S. Fotopoulos (2002), Stochastic incipient motion criterion for spheres under various bed packing conditions, *J. Hydraul. Eng.*, *128*(4), 369–380, doi:10.1061/(ASCE)0733-9429(2002)128:4(369).

Paphitis, D., and M. B. Collins (2005), Sand grain threshold, in relation to bed 'stress history': An experimental study, *Sedimentology*, *52*(4), 827–838, doi:10.1111/j.1365-3091.2005.00710.x.

Parker, C., N. J. Clifford, and C. R. Thorne (2011), Understanding the influence of slope on the threshold of coarse grain motion: Revisiting critical stream power, *Geomorphology*, *126*(1–2), 51–65, doi:10.1016/j.geomorph.2010.10.027.

Parker, G. (2007), Transport of gravel and sediment mixtures, in *Sedimentation Engineering: Theories, Measurements, Modeling and Practice*, *Manuals Rep. Eng. Practice*, vol. 110, edited by M. Garcia, pp. 165–252, Am. Soc. Civ. Eng., Reston, Va.

Parsons, A. J., and S. G. L. Stromberg (1998), Experimental analysis of size and distance of travel of unconstrained particles in interrill flow, *Water Resour. Res.*, *34*(9), 2377–2381, doi:10.1029/98WR01471.

Parsons, A. J., J. Wainwright, and A. D. Abrahams (1993), Tracing sediment movement in interrill overland-flow on a semiarid grassland hillslope using magnetic-susceptibility, *Earth Surf. Processes Landforms*, *18*(8), 721–732, doi:10.1002/esp.3290180806.

Parsons, A. J., J. Wainwright, A. D. Abrahams, and J. R. Simanton (1997), Distributed dynamic modelling of interrill overland flow, *Hydrol. Processes*, *11*(14), 1833–1859, doi:10.1002/(SICI)1099-1085(199711)11:14<1833::AID-HYP499>3.0.CO;2–7.

Parsons, A. J., S. G. L. Stromberg, and M. Greener (1998), Sediment-transport competence of rain-impacted interrill overland flow, *Earth Surf. Processes Landforms*, *23*(4), 365–375, doi:10.1002/(SICI)1096-9837(199804)23:4<365::AID-ESP851>3.0.CO;2–6.

Parsons, A. J., J. Wainwright, D. M. Powell, J. Kaduk, and R. E. Brazier (2004), A conceptual model for determining soil erosion by water, *Earth Surf. Processes Landforms*, *29*(10), 1293–1302, doi:10.1002/esp.1096.

Pavia, E. G., and B. Cushmanroisin (1988), Modeling of oceanic fronts using a particle method, *J. Geophys. Res.*, *93*(C4), 3554–3562, doi:10.1029/JC093iC04p03554.

Poesen, J. (1987), Transport of rock fragments by rill flow: A field study, *Catena Suppl.*, *8*, 35–54.

Quansah, C. (1981), The effect of soil type, slope, rain intensity and their interactions on splash detachment and transport, *J. Soil Sci.*, *32*(2), 215–224, doi:10.1111/j.1365-2389.1981.tb01701.x.

Rejman, J., B. Usowicz, and R. Debicki (1999), Source of errors in predicting silt soil erodibility with USLE, *Pol. J. Soil Sci.*, *32*, 13–22.

Riezebos, H. T., and G. F. Epema (1985), Drop shape and erosivity Part II: Splash detachment, transport and erosivity indexes, *Earth Surf. Processes Landforms*, *10*(1), 69–74, doi:10.1002/esp.3290100109.

Savat, J. (1981), Work done by splash: Laboratory experiments, *Earth Surf. Processes Landforms*, *6*(3–4), 275–283, doi:10.1002/esp.3290060308.

Savat, J., and J. Poesen (1981), Detachment and transportation of loose sediments by raindrop splash: Part I The calculation of absolute data on detachability and transportability, *Catena*, *8*, 1–17, doi:10.1016/S0341-8162(81)80001-X.

Schlichting, H. (1979), *Boundary-Layer Theory*, 6th ed., McGraw Hill, New York.

Schultz, M. P., and K. A. Flack (2003), Turbulent boundary layers over surfaces smoothed by sanding, *J. Fluid. Eng.*, *125*(5), 863–870.

Scoging, H. M. (1992), Modelling overland-flow hydrology for dynamic hydraulics, in *Overland Flow: Hydraulics and Erosion Mechanics*, edited by A. J. Parsons and A. D. Abrahams, pp. 89–104, Univ. Coll. London, London.

Scoging, H. M., A. J. Parsons, and A. D. Abrahams (1992), Application of a dynamic overland flow hydraulic model to a semi-arid hillslope, Walnut Gulch, Arizona, in *Overland Flow: Hydraulics and Erosion Mechanics*, edited by A. J. Parsons and A. D. Abrahams, pp. 105–145, Univ. Coll. London, London.

Shvidchenko, A. B., and G. Pender (2000), Flume study of the effect of relative depth on the incipient motion of coarse uniform sediments, *Water Resour. Res.*, *36*(2), 619–628, doi:10.1029/1999WR900312.

Smith, R. E., and J.-Y. Parlange (1978), A parameter-efficient hydrologic infiltration model, *Water Resour. Res.*, *14*, 533–538, doi:10.1029/WR014i003p00533.

Song, T., U. Lemmin, and W. H. Graf (1994), Uniform-flow in open channels with movable gravel-bed, *J. Hydraul. Res.*, *32*(6), 861–876, doi:10.1080/00221689409498695.

Su, B. L., S. Kazama, M. J. Lu, and M. Sawamoto (2003), Development of a distributed hydrological model and its application to soil erosion simulation in a forested catchment during storm period, *Hydrol. Processes*, *17*(14), 2811–2823, doi:10.1002/hyp.1435.

Syrjala, S. E. (1996), A statistical test for a difference between the spatial distributions of two populations, *Ecology*, *77*(1), 75–80, doi:10.2307/2265656.

Tachie, M. F., D. J. Bergstrom, and R. Balachandar (2000), Rough wall turbulent boundary layers in shallow open channel flow, *J. Fluid. Eng.*, *122*(3), 533–541.

Tatard, L., O. Planchon, J. Wainwright, G. Nord, D. Favis-Mortlock, N. Silvera, O. Ribolzi, M. Esteves, and C. H. Huang (2008), Measurement and modelling of high-resolution flow-velocity data under simulated rainfall on a low-slope sandy soil, *J. Hydrol.*, *348*(1–2), 1–12, doi:10.1016/j.jhydrol.2007.07.016.

Tisdall, J. M., and J. M. Oades (1982), Organic-matter and water-stable aggregates in soils, *J. Soil Sci.*, *33*(2), 141–163, doi:10.1111/j.1365-2389.1982.tb01755.x.

Torri, D. (1987), A theoretical-study of soil detachability, *Catena Suppl.*, *10*, 15–20.

Torri, D., and J. Poesen (1988), Incipient motion conditions for single rock fragments in simulated rill flow, *Earth Surf. Processes Landforms*, *13*(3), 225–237, doi:10.1002/esp.3290130304.

Torri, D., M. Sfalanga, and M. Delsette (1987), Splash detachment: Runoff depth and soil cohesion, *Catena*, *14*(1–3), 149–155, doi:10.1016/S0341-8162(87)80013-9.

Torri, D., R. Biancalani, and J. Poesen (1990), Initiation of motion of gravels in concentrated overland-flow: Cohesive forces and probability of entrainment, *Catena Suppl.*, *17*, 79–90.

Tsimplis, M. N. (1992), The effect of rain in calming the sea, *J. Phys. Oceanogr.*, *22*(4), 404–412, doi:10.1175/1520-0485(1992)022<0404:TEORIC>2.0.CO;2.

Tucker, G. E., and D. N. Bradley (2010), Trouble with diffusion: Reassessing hillslope erosion laws with a particle-based model, *J. Geophys. Res.*, *115*, F00A10, doi:10.1029/2009JF001264.

Turnbull, L., J. Wainwright, and R. E. Brazier (2010), Hydrology, erosion and nutrient transfers over a transition from semi-arid grassland to shrubland in the South-Western USA: A modelling assessment, *J. Hydrol.*, *388*(3–4), 258–272, doi:10.1016/j.jhydrol.2010.05.005.

Vanoni, V. A., and G. N. Nomicos (1960), Resistance properties of sediment-laden streams, *Trans. Am. Soc. Civ. Eng.*, *125*, 1140–1167.

van Rijn, L. C. (1984), Sediment transport, Part II: Suspended load transport, *J. Hydraul. Eng.*, *110*, 1613–1641, doi:10.1061/(ASCE)0733-9429(1984)110:11(1613).

Wainwright, J., and A. J. Parsons (2002), The effect of temporal variations in rainfall on scale dependency in runoff coefficients, *Water Resour. Res.*, *38*(12), 1271, doi:10.1029/2000WR000188.

Wainwright, J., and J. B. Thornes (1991), Computer and hardware simulations of archæological sediment transport, in *Computer Applications and Quantitative Methods in Archaeology 1990*, *BAR Int. Ser.*, vol. 565, edited by K. Lockyear and S. Rahtz, pp. 183–194, Archaeopress, Oxford, U. K.

Wainwright, J., A. J. Parsons, and A. D. Abrahams (1995), A simulation study of the role of raindrop erosion in the formation of desert pavements, *Earth Surf. Processes Landforms*, *20*(3), 277–291, doi:10.1002/esp.3290200308.

Wainwright, J., A. J. Parsons, and A. D. Abrahams (1999), Rainfall energy under creosotebush, *J. Arid Environ.*, *43*(2), 111–120, doi:10.1006/jare.1999.0540.

Wainwright, J., A. J. Parsons, E. N. Muller, R. E. Brazier, D. M. Powel, and B. Fenti (2008a), A transport-distance approach to scaling erosion rates: 1. Background and model development, *Earth Surf. Processes Landforms*, *33*(5), 813–826, doi:10.1002/esp.1624.

Wainwright, J., A. J. Parsons, E. N. Muller, R. E. Brazier, D. M. Powell, and B. Fenti (2008b), A transport-distance approach to scaling erosion rates: 2. Sensitivity and evaluation of MAHLERAN, *Earth Surf. Processes Landforms*, *33*(6), 962–984, doi:10.1002/esp.1623.

Wainwright, J., A. J. Parsons, E. N. Muller, R. E. Brazier, D. M. Powell, and B. Fenti (2008c), A transport-distance approach to scaling erosion rates: 3. Evaluating scaling characteristics of MAHLERAN, *Earth Surf. Processes Landforms*, *33*(7), 1113–1128, doi:10.1002/esp.1622.

Wells, R. R., C. V. Alonso, and S. J. Bennett (2009), Morphodynamics of headcut development and soil erosion in upland concentrated flows, *Soil Sci. Soc. Am. J.*, *73*(2), 521–530, doi:10.2136/sssaj2008.0007.

Wilcock, P. R. (1997), The components of fractional transport rate, *Water Resour. Res.*, *33*(1), 247–258, doi:10.1029/96WR02666.

Wilcock, P. R., and B. W. McArdell (1997), Partial transport of a sand/gravel sediment, *Water Resour. Res.*, *33*(1), 235–245, doi:10.1029/96WR02672.

Wilcock, P. R., A. F. Barta, C. C. Shea, G. M. Kondolf, W. V. G. Matthews, and J. Pitlick (1996), Observations of flow and sediment entrainment on a large gravel-bed river, *Water Resour. Res.*, *32*(9), 2897–2909, doi:10.1029/96WR01628.

Wilcock, P. R., S. T. Kenworthy, and J. C. Crowe (2001), Experimental study of the transport of mixed sand and gravel, *Water Resour. Res.*, *37*(12), 3349–3358, doi:10.1029/2001WR000683.

Wood, E. F., M. Sivapalan, K. Beven, and L. Band (1988), Effects of spatial variability and scale with implications to hydrologic modeling, *J. Hydrol.*, *102*(1–4), 29–47, doi:10.1016/0022-1694(88)90090-X.

Woolhiser, D. A., R. E. Smith, and D. C. Goodrich (1990), *KINEROS, a Kinematic Runoff and Erosion Model: Documentation and user manual*, *Agric. Res. Serv. Publ.*, vol. 77, U.S. Dep. of Agric., Washington, D. C.

Wright, A. C. (1987), A model of the redistribution of disaggregated soil particles by rainsplash, *Earth Surf. Processes Landforms*, *12*(6), 583–596, doi:10.1002/esp.3290120602.

Wu, F. C., and Y. C. Lin (2002), Pickup probability of sediment under log-normal velocity distribution, *J. Hydraul. Eng.*, *128*(4), 438–442, doi:10.1061/(ASCE)0733-9429(2002)128:4(438).

Zhang, Q. W., T. W. Lei, and J. Zhao (2008), Estimation of the detachment rate in eroding rills in flume experiments using an REE tracing method, *Geoderma*, *147*(1–2), 8–15.